New Phytologist

Research

Defender or accomplice? Dual roles of plant vesicle trafficking in restricting and enabling geminiviral systemic infection

Pepe Cana-Quijada[1]*, Pablo Morales-Martínez[1]*, Tábata Rosas-Díaz[1], Jessica Pérez-Sancho[1], Tamara Jiménez-Góngora[1], José Antonio Navarro[2], Rosa Lozano-Durán[3], Araceli G. Castillo[1], Vicente Pallás[2] and Eduardo R. Bejarano[1]

[1]Instituto de Hortofruticultura Subtropical y Mediterránea "La Mayora" (IHSM "La Mayora"), Unidad de Protección de Cultivos, Universidad de Málaga-Consejo Superior de Investigaciones Científicas (UMA-CSIC), Campus Teatinos, 29010, Málaga, Spain; [2]Instituto de Biología Molecular y Celular de Plantas (IBMCP), Universitat Politècnica de València-Consejo Superior de Investigaciones Científicas, Ingeniero Fausto Elio s/n, 46022, Valencia, Spain; [3]Department of Plant Biochemistry, Center for Plant Molecular Biology (ZMBP), Eberhard Karls University, 72076, Tübingen, Germany

Author for correspondence:
Eduardo R. Bejarano
Email: edu_rodri@uma.es

Received: *15 May 2025*
Accepted: *29 September 2025*

New Phytologist (2025)
doi: 10.1111/nph.70707

Key words: clathrin-mediated transport, COPI complex, endomembrane system, geminiviruses, plant–virus interactions, vesicle trafficking.

Summary

- The vesicle trafficking system enables multidirectional cargo fluxes between endomembrane compartments. However, vesicle trafficking plays dual roles during pathogen infections. In plants, it mediates autophagic immune responses but can also be hijacked by pathogens to facilitate successful infections.
- We demonstrate that vesicle trafficking machinery acts as a double-edged sword during infection by the geminivirus tomato yellow leaf curl Sardinia virus (TYLCSaV) in *Nicotiana benthamiana*. Virus-induced gene silencing of eight genes encoding key vesicle trafficking regulators revealed contrasting outcomes. Silencing of *NbSAR1* and *NbAP-1*γ significantly increased systemic geminiviral DNA accumulation, whereas silencing of *Nb*δ*-COP*, *NbARF1* and clathrin genes almost completely abolished infection. Notably, this inhibition is hypothesized to result from direct or indirect impairment in viral movement, as replication remained unaffected by gene silencing.
- The observed effects affect other geminiviruses, including tomato yellow leaf curl virus (TYLCV) and beet curly top virus (BCTV), but not unrelated pathogens, such as the RNA potato virus X (PVX) or the plant pathogenic bacterium *Pseudomonas syringae*.
- These findings suggest that while the vacuolar and autophagy branches of the vesicle trafficking system might mediate antiviral autophagic defence responses, the integrity of endocytosis and retrograde transport is essential for systemic geminiviral infection.

Introduction

Vesicle trafficking constitutes a complex network of transport pathways between organelles and membranes within eukaryotic cells that allows the preservation of each subcellular compartment identity, viability and function. Despite the ravishing complexity of vesicle trafficking in eukaryotes, major routes are conserved across the *Eukarya* domain, although distinct organizational traits are found between species. Thus, the most extensively described pathways in mammals and yeasts have also been thoroughly characterized in plants mainly comprising: (1) endoplasmic reticulum (ER)–Golgi apparatus (hereafter referred to as Golgi) interface, (2) the trafficking between *trans*-Golgi network (TGN) and plasma membrane (PM) and (3) vacuolar transport. ER–Golgi interface trafficking mediates bidirectional communication between these organelles through anterograde and retrograde routes. TGN–PM crossroads involve both secretory and endocytic pathways. Finally, vacuolar transport involves both TGN maturation to constitute multivesicular bodies/prevacuolar compartments (MVB/PVC) and their fusion to the vacuole or the PM (Fig. 1; reviewed in Hu *et al.*, 2020; Aniento *et al.*, 2022; González Solís *et al.*, 2022; Zeng *et al.*, 2023; Cadena-Ramos & De-la-Peña, 2024).

Vesicular transport orchestrates the formation, movement and fusion of vesicles from donor organelles to their target membranes. This process begins with membrane deformation, which facilitates the budding and scission of vesicles from their originating compartments. Once released, vesicles traverse the cytosol either through free diffusion or via interactions with cytoskeletal elements, which guide and propel them towards their destinations. Upon reaching their target membranes, vesicles dock and fuse, ensuring the precise delivery of their cargo to maintain cellular functionality and compartmental integrity. Such a complex process requires regulation and specificity given by an array of

*These authors contributed equally to this work.

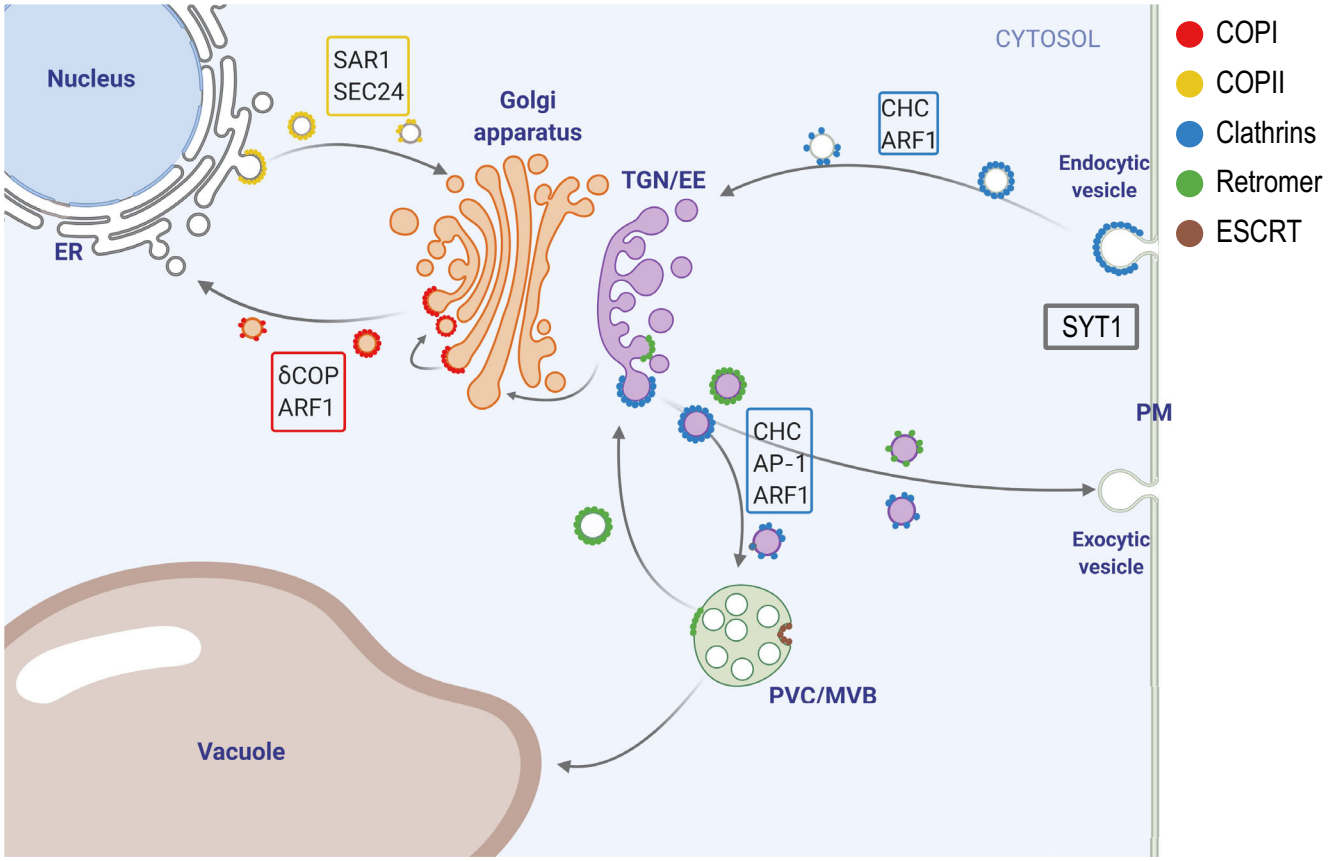

Fig. 1 Location of the selected factors in the different endomembrane system pathways. The genes selected in this study (shown in boxes) are placed next to the routes in which they participate using the same colour code used to represent the different vesicle coatings. *δ-COP* and *ARF1* were selected to interrupt the retrograde pathway, *SAR1* and *SEC24* to interrupt the anterograde pathway, *CHC1* and *CHC2* for every pathway in which clathrins intervene and *AP-1* for the TGN)-to-PVC/MVB and secretory routes. Even though *SYT1* is not involved in specific vesicle trafficking pathways, it allows membrane contact site formation between the ER and the PM. Vesicle outlines indicate the specific set of coat proteins involved in forming each type of vesicle: COPI for retrograde Golgi-to-ER pathway, COPII for anterograde ER-to-Golgi pathway, clathrins for most of the post-Golgi trafficking, retromer complexes for recycling routes and ESCRT (Endosomal Sorting Complex Required for Transport) proteins for the budding of intraluminal vesicles within MVBs. *ARF1*, ADP-ribosylation factor 1; *CHC*, Clathrin Heavy Chain; COP, Coat Protein Complex; EE, early endosome; ER, endoplasmic reticulum; PM, plasma membrane; PVC/MVB, prevacuolar compartment/multivesicular body; *SAR1*, Secretion-associated RAS 1; *SYT1*, Synaptotagmin1; TGN, *Trans*-Golgi Network.

factors (such as coat GTPases or vesicle coat proteins) present in each organelle, whose different combinations will give rise to each particular vesicle and define each of the aforementioned vesicular pathways (Aniento *et al.*, 2022; Gao & Chao, 2022; Li *et al.*, 2022). Coat GTPases function as molecular switches eliciting the recruitment of cargoes and vesicle structural proteins. All described coat GTPases are classified into the family of small GTPases named secretion-associated RAS (SAR) and ADP-ribosylation factor (ARF), the SAR/ARF family (Yorimitsu *et al.*, 2014; Jackson *et al.*, 2023). Five different SAR1 genes have been identified in the *Arabidopsis thaliana* (hereafter referred to as Arabidopsis) genome, named SAR1A-E (Brandizzi, 2018), that mediate ER-to-Golgi anterograde transport (Van der Verren & Zanetti, 2023). On the contrary, at least nine ARF proteins have been characterized in Arabidopsis. Six of them are orthologous to the mammalian class-I ARFs (ADP-ribosylation factor 1 (ARF1); Vernoud *et al.*, 2003; Gebbie *et al.*, 2005; Muthamilarasan *et al.*, 2016; Singh & Jürgens, 2018) and participate in various pathways: (1) Golgi-to-ER retrograde trafficking (Lee *et al.*, 2002; Takeuchi *et al.*, 2002), (2) endocytosis and/or recycling pathways (Xu & Scheres, 2005; Naramoto *et al.*, 2010; Tanaka *et al.*, 2014) and (3) vacuolar trafficking (Pimpl *et al.*, 2003). Moreover, vesicle coat proteins encompass both adaptor proteins, involved in cargo recognition, and cage proteins, conferring structural support and specificity for vesicle docking. The Coat Protein Complex II (COPII) components are required for anterograde transport from the ER to the Golgi, whereas retrograde transport from the Golgi to the ER is mediated by the COPI complex. COPII vesicles require the assembly of SAR1 GTPase, the adaptor complex SEC23/SEC24 and the cage complex SEC13/SEC31. On the contrary, formation of COPI vesicles involves the recruitment of ARF1 GTPases and seven subunits of coat proteins assembled *en bloc*: α-, β-, β'-, γ-, δ-, ε- and ζ-COP (Brandizzi & Barlowe, 2013; Luo & Boyce, 2019; Aniento *et al.*, 2022; Li *et al.*, 2022). Vesicles covering the exocytic and endocytic pathways, as well as vacuolar

transport, require the action of ARF GTPases and are coated by two subsets of proteins: adaptor complexes (e.g. adaptor protein 1 (AP-1) complex) and the cage-forming proteins named clathrins. The latter give name to these vesicles: clathrin-coated vesicles (CCVs; Fig. 1; Law *et al.*, 2022; Shimizu & Uemura, 2022).

The endomembrane trafficking system also entails an important source of components and pathways for viruses to co-opt for their own benefit (Yuen *et al.*, 2023). Plant RNA viruses make use of this system for cell-to-cell movement and the formation of viral replication complexes (VRCs). Frequently, these processes rely on molecular interactions between components of the vesicle trafficking pathways and viral movement proteins (MPs; Pitzalis & Heinlein, 2017; Navarro *et al.*, 2019; Rodriguez-Peña *et al.*, 2021). Geminiviruses are circular single-stranded (ss) DNA viruses of small size (from 2.5 to 3.0 kb) that constitute the largest plant DNA viral family. Among them, the *Begomovirus* genus is the best characterized and comprises > 450 species that are transmitted by the whitefly *Bemisia tabaci* (Fiallo-Olivé *et al.*, 2021; Fiallo-Olivé & Navas-Castillo, 2023). Geminiviruses replicate in the nucleus of infected plant cells, utilizing the host DNA polymerases α and δ (Wu *et al.*, 2021). Unlike many other viruses, geminiviruses have not been reported to induce significant remodelling of the host endomembrane system for their replication or movement within the plant host. However, several pieces of evidence suggest the relevance of the endomembrane trafficking system during geminivirus infection. Interactions of geminiviral proteins, including MPs and nuclear shuttle proteins (NSPs), and plant proteins involved in post-Golgi clathrin-mediated trafficking (STOMATAL CYTOKINESIS DEFECTIVE, SCD2), endocytosis and ER–PM contact sites tethering (Synaptotagmin1, SYT1) or nuclear export of NSP–viral DNA complex to plasmodesmata (NSP-interacting GTPase, NIG1) have been described (Carvalho *et al.*, 2008; Krapp *et al.*, 2017). Based on the presence of viral DNA and geminivirus movement-related proteins (MP and the NSP) in endosomes (Lewis & Lazarowitz, 2010), Gouveia-Mageste *et al.* (2021) proposed a model in which interactions between NSP and the plant syntaxin protein NISP regulate the intracellular trafficking of vDNA to endosomes. At this site, MP – recruited from the PM by the endosomal protein SYTA – opportunistically associates with the NSP–vDNA complex to mediate cell-to-cell movement through an endocytic recycling pathway that redirects the complex back to the plasmodesmata. Moreover, intercellular movement of the begomovirus cabbage leaf curl virus (CabLCV) is reduced in infected *syt1* mutant plants, as it was also observed for several species of tobamoviruses and potyviruses (Uchiyama *et al.*, 2014; Cabanillas *et al.*, 2018). Excitingly, the relevance of vesicle trafficking for geminiviral movement has even been demonstrated within their insect viral vectors, as the begomoviruses tomato yellow leaf curl virus (TYLCV) and cotton leaf curl Multan virus (CLCuMuV) have been shown to accumulate in vesicle-like structures inside *Bemisia tabaci* cells that cross the whitefly midgut through clathrin-mediated endocytosis (Pan *et al.*, 2017; Chi *et al.*, 2021).

Using a combination of virus-induced gene silencing (VIGS) and transgenic *Nicotiana benthamiana* reporter plants that contain a GFP (Green Fluorescence Protein) transgene whose expression is dependent on the viral replication (*2IRGFP* plants, Morilla *et al.*, 2006), we previously demonstrated that the δ-COP subunit of the COPI complex is required for viral infection (Lozano-Durán *et al.*, 2011). In this study, we further characterized different pathways of the plant endomembrane trafficking system by silencing specific components and analysing their effects on the localization of Golgi, TGN and MVB markers. Moreover, our results showed that some vesicle trafficking elements, such as SAR1 or AP-1γ, play antiviral roles during geminivirus infection while, in addition to δ-COP, the expression of *ARF1* and *Clathrin heavy chain 1* and *2* (*CHC1* and *CHC2*) is essential for geminivirus infection, but not for other pathogens, such as RNA viruses or bacteria. Hence, this work highlights the dual role of the vesicle trafficking system in maintaining cellular function and mediating susceptibility to geminiviruses.

Materials and Methods

Microorganisms: bacterial strains and infectious clones

Manipulation of bacteria was performed according to standard methods (Ausubel *et al.*, 1998; Sambrook & Russell, 2001). *Escherichia coli* strain DH5α was used for cloning procedures. *Agrobacterium tumefaciens* strain GV3101 allowed the delivery of tobacco rattle virus (TRV) RNA2-based vectors and the infective clones of tomato yellow leaf curl Sardinia virus (TYLCSaV) (GenBank accession: L27708) and beet curly top virus (BCTV) (GenBank accession: NC001412), whereas strain LBA4404 was employed for the delivery of the infectious clone of tomato yellow leaf curl virus (TYLCV) (GenBank accession: AJ489258) and strain C58 was used for the transient expression of fluorescence proteins in *N. benthamiana* Domin.

Plant material and growth conditions

Nicotiana benthamiana Domin wild-type and *2IRGFP* plants (Morilla *et al.*, 2006) were grown in controlled growth chambers at 24°C under 16 h : 8 h, light : dark long-day conditions.

Plasmids and cloning

Candidate genes for the VIGS constructs were introduced into VIGS Tool (solgenomics.net) and 300-bp regions were selected and amplified by specific primers from *N. benthamiana* cDNA (Supporting Information Table S1). Amplified fragments were cloned into pGEMT-easy (Promega) and sequenced. pGEMT clones were digested with *Spe*I and *Apa*I restriction enzymes (Takara), and the corresponding fragments were subcloned into *Spe*I/*Apa*I sites of the TRV RNA2-based vector pTV00 (Ratcliff *et al.*, 2001), yielding the correspondent TRV-derived VIGS constructs used to silence the selected vesicle trafficking plant genes (Table 1).

Virus-induced gene silencing

VIGS assays in *N. benthamiana* plants were performed using TRV according to the method described in Ratcliff *et al.* (2001). Different cultures of *A. tumefaciens* harbouring pTV00 or

Table 1 Selected genes used to test the impact of the vesicle trafficking in geminiviral infection.

Silenced genes	Pathway	Function	Arabidopsis locus
δ-COP	Golgi-to-ER retrograde transport, intra-Golgi transport	COPI complex subunit	At5g05010
ARFA1B	Golgi-to-ER retrograde transport, intra-Golgi transport, post-Golgi trafficking	Small GTPase essential for COPI and clathrin-coated vesicles (CCVs) formation	At5g14670
SAR1B	ER-to-Golgi anterograde pathway	Small GTPase essential for COPII vesicle formation	At1g56330
SEC24A	ER-to-Golgi anterograde pathway	Structural coat protein of COPII vesicles	At3g07100
SYT1	Membrane contact sites	ER-PM tethering. Impacts over geminiviral infection	At2g20990
AP-1γ	Vacuolar trafficking from the TGN	AP-1γ complex subunit and structural component of CCVs	At1g60070
CHC1	Post-Golgi trafficking, endo-exocytosis	Structural component of CCVs	At3g11130
CHC2	Post-Golgi trafficking, endo-exocytosis	Structural component of CCVs	At3g08530

Selected genes from different vesicle trafficking routes to be silenced by virus-induced gene silencing (VIGS). Pathway involvement, function and *loci* of the *Arabidopsis thaliana* selected genes are indicated. *AP-1*. adaptor protein 1; *ARF1*, ADP-ribosylation factor 1; *CHC*, Clathrin Heavy Chain; *COP*, Coat Protein Complex; ER, endoplasmic reticulum; *SAR1*, Secretion-associated RAS 1; *SYT1*, Synaptotagmin1; TGN, Trans-Golgi Network.

pTV00-derived constructs and an independent culture of *A. tumefaciens* carrying pBINTRA6 were liquid-cultured in LB (Lysogeny broth) overnight with appropriate antibiotics. The cultures were then prepared for agroinfiltration at an OD_{600} = 1. A 1 : 1 mixture was done with the pBINTRA6 culture and the pTV00 or pTV00-derived cultures. Mixed cell cultures were infiltrated in the underside of two leaves of 4-wk-old *N. benthamiana* plants. In certain experiments, the plants were also infected with geminiviruses at the same time as described below.

Specific primers to evaluate the silencing efficiency of the TRV constructs are shown in Table S1. Sequence alignment between primers and cDNA sequences of the family members allowed us to estimate which transcripts could be measured and amplified by qPCR (Table 2).

Geminivirus systemic infection assays

Five-week-old *2IRGFP N. benthamiana* plants were agroinoculated with the infectious clones of TYLCSaV (Lozano-Durán *et al.*, 2011), TYLCV (Morilla *et al.*, 2005) or BCTV (Briddon *et al.*, 1989) according to previously described methods (Elmer *et al.*, 1988). In brief, *A. tumefaciens* carrying the respective infectious clones were grown on liquid LB medium supplemented with the appropriate antibiotics overnight. Bacterial cultures were centrifuged at 4000 ***g*** for 10 min and resuspended in agroinoculation buffer (10 mM $MgCl_2$, 10 mM MES pH 5.6, and 100 μM acetosyringone), the optical density being adjusted to 1 (OD_{600} = 1).

Between 2 and 4 h after incubation in the dark at room temperature, bacterial cultures were inoculated in the axillary bud of the fourth/fifth leaf of the plants using a syringe with a needle. After 15 d, samples were collected and processed for DNA and RNA isolation.

Geminivirus replication assay

The second and third leaves of *2IRGFP N. benthamiana* plants inoculated with empty TRV control or silenced using VIGS were agroinoculated with the TYLCSaV infectious clone (pGTYA14) 7 d after TRV constructs infiltration using a needleless syringe and following the same agroinfiltration method as described above with an OD_{600} = 0.5. Four days later, the infiltrated leaves were sampled and processed for DNA and RNA isolation.

PVX infection assays

Potato virus X (PVX)-GFP was kindly provided by Dr. Peter Moffett and previously used in Peart *et al.* (2002); Jaubert *et al.* (2011). *N. benthamiana* plants were agroinoculated at an OD_{600} = 0.01 at 7 d postinoculation (dpi) after TRV constructs inoculation. Leaf samples were taken at 15 dpi, and total RNA was extracted from the three apical leaves of each infected *N. benthamiana* plant. For quantification of PVX-GFP, virus-derived GFP expression was assessed by real-time PCR as described below.

Pseudomonas syringae inoculation and growth assays

Ten days after the inoculation with TRV-silencing constructs, the leaves from both silenced and control plants were infiltrated with the bacteria. *Pseudomonas syringae* pv tomato DC3000 cultures (Cuppels, 1986) were grown at 28 °C in LB medium supplemented with the proper antibiotics. Bacteria were suspended in agroinoculation buffer (as described in the previous section). Two leaves of 4- to 5-wk-old *N. benthamiana* plants were inoculated by infiltrating a 5×10^4 colony-forming units (CFU) ml^{-1} bacterial suspension using a needleless syringe. Samples were taken from inoculated leaves at 0 and 3 dpi and homogenized in 10 mM $MgCl_2$ by mechanical disruption. Serial dilutions of the resulting bacterial suspensions were plated onto LB plates supplemented with cycloheximide (2 μg ml^{-1}) and rifampicin (15 μg ml^{-1}) to determine the bacterial count (CFU ml^{-1}).

Nucleic acids isolation

Plant total DNA was extracted from *N. benthamiana* leaves (from infiltrated leaves for replication assays and from apical leaves in systemic infection assays) following the CTAB method as

Table 2 Vesicle trafficking-related genes targeted for silencing.

G.O.I.	*Arabidopsis thaliana* selected gene	*Nicotiana benthamiana* genes	Predicted silencing	Putatively detected by RT-qPCR	Plant phenotype
δ-COP	At5g05010	**Niben101Scf09552g01014**	✓[1]	✓	Stunted, wrinkled and curved apical leaves
		Niben101Scf08334g03001	✓[1]	✓	
ARFA1B	At5g14670	**Nbv6.1trP74299***	✓	✓	Stunted, wrinkled and curved apical leaves
		Nbv6.1trP47890*	✓	✓	
SAR1B	At1g56330	**Niben101Scf02693g00001**	✓	✓	None
		Niben101Scf01623g17008	✓	✓	
		Niben101Scf00332g05012			
		Niben101Scf04473g02002			
		Niben101Scf00466g04034			
		Niben101Scf07576g00030			
		Niben101Scf05336g00011	✓		
		Niben101Scf09612g00005			
		Niben101Scf05099g00008			
		Niben101Scf09203g01012			
		Niben101Scf04819g02004	✓		
SEC24A	At3g07100	**Niben101Scf06077g05012**	✓	✓	None
		Niben101Scf07027g02001			
SYT1	At2g20990	**Niben101Scf02025g03007**	✓	✓	None
		Niben101Scf07109g01003	✓		
AP-1γ	At1g60070	**Niben101Scf08728g01001**	✓	✓	None
		Niben101Scf01053g01016	✓	✓	
		Niben101Scf03099g00001	✓		
		Niben101Scf06734g01028	✓		
CHC1	At3g11130	**Niben101Scf05954g03005**	✓	✓	Stunted, wrinkled and curved apical leaves
		Niben101Scf03779g01005	✓	✓	
CHC2	At3g08530	**Niben101Scf10169g04008**	✓	✓	Stunted, wrinkled and curved apical leaves
		Niben101Scf01237g01011	✓	✓	
		Niben101Scf01200g02001	✓	✓	
		Niben101Scf10519g01006	✓	✓	

Selected *Arabidopsis thaliana loci* served as reference sequences in outlining *Nicotiana benthamiana* homologue gene family, annotated using SolGenomics accession codes. Bold marks the putative *N. benthamiana* orthologue. *NbARFA1B* genes, marked with (*), are referenced from QUT database (Ranawaka *et al*., 2023) due to incomplete annotation in SolGenomics. *N. benthamiana* genes *in silico* predicted to be silenced and/or measured by RT-qPCR are shown and silenced plant phenotypes are briefly described.
[1]*In silico* predicted silencing allowing at least 1 mismatch in VIGS-Tool (SolGenomics). *AP-1*. adaptor protein 1; *ARF1*, ADP-ribosylation factor 1; *CHC*, Clathrin Heavy Chain; *COP*, Coat Protein Complex; *SAR1*, Secretion-associated RAS 1; *SYT1*, Synaptotagmin1.

described in Lukowitz *et al.* (1996). Briefly, *c.* 50–100 mg of plant macerated tissue was homogenized into 500 µl of extraction buffer (2% cetyl trimethylammonium bromide (CTAB), 1.5 M NaCl, 100 mM Tris pH 8, 100 mM EDTA pH 8) and incubated at 65°C for 15 min. After cooling, the mixture was extracted with chloroform/isoamyl alcohol (24 : 1) and the nucleic acids were precipitated with isopropanol. DNA was finally resuspended in water and treated with RNase (10 mg ml^{-1}; Invitrogen).

RNA extractions were performed according to the phenol-free method described by Oñate-Sánchez & Vicente-Carbajosa (2008). Approximately 50–100 mg of plant tissue was homogenized into 300 µl of cell lysis buffer (2% sodium dodecyl sulphate (SDS), 68 mM sodium citrate, 132 mM citric acid, 1 mM ethylenediaminetetraacetic acid (EDTA) pH 8). One hundred microlitres of protein–DNA precipitation solution (4 M NaCl, 16 mM sodium citrate and 32 mM citric acid) was added to the cell lysate, and the mixture was incubated on ice for 10 min. The samples were centrifuged at 4°C for 10 min, and supernatants were transferred to new tubes for isopropanol precipitation as previously described.

Quantitative real-time PCR (qPCR) and reverse transcription qPCR (RT-qPCR)

cDNA was synthesized using iScript™ cDNA Synthesis Kit (Bio-Rad) following the instructions provided by the manufacturer.

Quantitative PCR was performed to quantify viral accumulation and measure transcript levels. Ten microlitres of reactions were prepared containing 1–10 ng of genomic DNA or cDNA as template, specific primers at 10 µM (Table S1) and 5 µl of SsoFast EvaGreen Supermix (Bio-Rad). The reactions were carried out in the CFX96 and CFX384 Touch Real-Time PCR Detection System instrument (Bio-Rad) following 10 min at 95°C and 40 cycles of 15 s at 95°C and 10 s at 60°C. Three technical replicates per sample were included in each reaction plate. The data were analysed using Livak's 2-DDCT method (Livak & Schmittgen, 2001).

Confocal laser scanning microscopy

To evaluate the effect of individual gene silencing on organelle markers, *Agrobacterium tumefaciens* cultures harbouring the

binary vectors expressing STtmd-GFP, SYP41-GFP and BP80-GFP, and were adjusted to an OD600 of 0.25 and agroinfiltrated into the leaves of *N. benthamiana* plants previously subjected to VIGS. The infiltrations of the markers were performed 11 d after infection with TRV-VIGS constructs.

In every case, fluorescence was detected in epidermal cells 2 d after infiltration using an inverted Zeiss LSM780 or Zeiss LSM880 confocal microscope (Zeiss, http://www.zeiss.com). GFP fluorescence was visualized by 488 nm excitation with an argon laser and its emission examined with a band-pass filter for 500–530 nm. Cortical plane images are maximum z-projections of several planes (1 mm spacing) from the cell surface to the cell equatorial plane.

Image analysis of organelle markers in silenced *N. benthamiana* leaves

Two-dimensional, max-intensity, z-projections of the z-stacks were made using the Fiji software (https://fiji.sc/; Schindelin *et al.*, 2012). Images were inspected, and the most general behaviour of each organellar marker (i.e. STtmd-GFP, SYP41-GFP and BP80-GFP) in response to each gene silencing was extracted. Representative images were selected and subjected to basic treatment in Fiji (brightness/contrast enhancement, smoothing) just for display purposes. The conditions where changes in the localization of the organellar markers were clear (STtmd-GFP and SYP41-GFP) were selected for further image analysis to quantify those changes.

For the analysis of BP80 marker signal, images were segmented using the interactive machine learning and segmentation software Ilastik (https://www.ilastik.org/; Berg *et al.*, 2019) to quantify the size of puncta. Five images were used for training, with all sigma values selected for all features. Training was based on three labels: background, defined puncta and blurry cytosolic-like signal. The colour-coded probability maps were generated and subsequently treated with Fiji for puncta analysis. A colour threshold was applied (min Hue = 34, max Hue = 132; min Brightness = 136, max Brightness = 255) to generate binary segmentation images. Then, particles were analysed to extract the list of puncta and their sizes (area) for each image. All image analysis data were represented as bar charts and histograms using GraphPad Prism v.10.4.1.

CFDA phloem transport assays

Phloem transport was assessed by infiltrating 100 µl of 500 µM 5(6)-carboxyfluorescein diacetate (CFDA; Sigma-Aldrich) into the abaxial surface of mature source leaves (fifth leaf from the apex) using a needleless syringe. Transport to both source and sink tissues (second leaf from the apex) was observed after 3 h of CFDA application in *δ-COP*-, *ARF1*-silenced and TRV control plants at 9 dpi.

Transversal sections of petioles from source and sink leaves were obtained using an epifluorescence stereomicroscope under (1) visible light, (2) ultraviolet (UV) light (450–490 nm) using a band-pass filter (500–575 nm) to visualize CFDA signal (green) and (3) a long-pass filter (> 500 nm) allowing simultaneous detection of CFDA fluorescence (green) and Chl autofluorescence (red).

Statistical analysis

Comparisons between experimental conditions and TRV controls were evaluated for statistically significant differences according to standard unpaired Student's *t*-tests (****, *P*-value < 0.0001; ***, *P*-value < 0.001; **, *P*-value < 0.01; *, *P*-value < 0.05).

Results

Identification of *N. benthamiana* orthologues of selected *A. thaliana* vesicle trafficking-related genes

To investigate the role of the vesicle trafficking system in geminiviral infection, we silenced key components of the vesicle trafficking machinery using the reverse genetic approach previously established by our group (Lozano-Durán *et al.*, 2011). Considering the complexity of the endomembrane pathway, which involves numerous genes in Arabidopsis, we selected specific genes to target distinct vesicle trafficking routes (Fig. 1; Table 1): (1) Golgi-to-ER retrograde pathway by silencing *δ-COP* and *ARF1* (also involved in post-Golgi trafficking), (2) ER-Golgi anterograde trafficking by targeting *SEC24* and *SAR1* and (3) post-Golgi routes encompassing trafficking pathways between the TGN, the vacuole and the PM by impairing the expression of *SYT1*, *AP-Iγ*, *CHC1* and *CHC2*.

VIGS constructs to silence *δ-COP* and *ARF1* in *N. benthamiana* have been previously described (Coemans *et al.*, 2008; Lozano-Durán *et al.*, 2011). For the remaining genes, we performed a bioinformatic analysis to identify *N. benthamiana* orthologues of the selected Arabidopsis genes, following the workflow outlined in Fig. S1. The cDNA and protein sequences of the Arabidopsis genes were used to launch a Blast search in the Sol Genomics Network database (solgenomics.net). Genes with the highest nucleotide and protein sequence homology scores were considered orthologues and were selected to design the VIGS constructs (Figs S2A–S9A). When discrepancies occurred between BlastP and BlastN results, candidate genes were refined through reverse BlastP, sequence conservation, gene family context and functional annotation. In cases where multiple Arabidopsis orthologs with very similar score of homology were retrieved, additional BlastP searches were performed using the identified *N. benthamiana* protein sequences as queries against the Arabidopsis database. To complete the study and assess the composition and complexity of the gene families, we performed a phylogenetic analysis of all selected genes using the Sol Genomics Network database, except for *ARF1* for which we resorted to the QUT database (Ranawaka *et al.*, 2023) due to incomplete annotation in Solgenomics (Figs S2B–S9B). Given the allotetraploid nature of *N. benthamiana* and the fact that many of the genes involved in vesicular trafficking are part of large gene families, special care was taken in designing the VIGS constructs in order to reduce the expression of many paralogues of each of the selected genes.

Table 3 Subcellular relocalization of endomembrane system upon silencing of vesicle trafficking elements.

Silenced genes	STtmd-GFP (Golgi)	SYP41-GFP (TGN)	BP80-GFP (MVB)
Control	Golgi	TGN	Multivesicular bodies (MBV)
δ-COP	Relocated at ER	Not altered	Not altered
ARFA1B	Relocated at ER	Not altered	Not altered
SAR1B	Relocated at ER	TGN localization lost	Severe changes. Located mainly at ER. Larger foci
SEC24A	Relocated at ER	Not altered	Not altered
AP-1γ	Mainly relocated at ER	Not altered	Localization severely altered. Larger foci
CHC2	Slightly relocated at ER	Not altered	Affected the integrity of the MVB. Larger foci

Impact in the localization of Golgi apparatus (STtmd-GFP), Trans-Golgi Network (SYP41-GFP) and Multivesicular bodies (BP80-GFP) markers in the silenced *Nicotiana benthamiana* plants. *AP-1*. adaptor protein 1; *ARF1*, ADP-ribosylation factor 1; *CHC*, Clathrin Heavy Chain; *COP*, Coat Protein Complex; ER, endoplasmic reticulum; *SAR1*, Secretion-associated RAS 1; *SYT1*, Synaptotagmin1; TGN, Trans-Golgi Network.

VIGS constructs to silence *SAR1*, *SEC24*, *SYT1*, *AP-1γ*, *CHC1* and *CHC2* were designed according to the flow chart outlined in Fig. S10. cDNA sequences of *N. benthamiana* orthologues of each gene family were analysed using the 'VIGS tool' from the Sol Genomics Network database to select a 300-bp fragment (RNA_{VIGS}) for each sequence. These fragments were chosen based on their ability to target the highest number of family members for each selected gene with high specificity while avoiding off-target effects outside the gene family. To predict the potential silencing efficiency across transcripts within each gene family, the 'VIGS tool' software was employed to calculate the number of predicted 21-mers generated from the RNA_{VIGS} fragments that would target these transcripts. Additionally, the percentage of nucleotide identity between the target sequences and the corresponding RNA_{VIGS} fragment was determined using the ClustalW alignment tool from the European Bioinformatics Institute (EBI, ebi.ac.uk; Figs S2B–S9B).

To further confirm that the selected fragments did not have obvious undesired off-targets, the RNA_{VIGS} fragments were used as queries for Blast searches on the *N. benthamiana* cDNA library (Fig. S10). The fragments that putatively only targeted the gene or gene family of interest were selected, PCR-amplified and cloned into the TRV RNA2-based VIGS vector, pTV00 (Ratcliff *et al.*, 2001). The silencing specificity and efficiency of TRV constructs *in silico* are shown in Figs S2C–S9C and Table 2.

Phenotype of plants silenced in elements of the plant endomembrane trafficking system

Silencing of *SAR1*, *SEC24*, *SYT1* and *AP-1γ* did not result in detectable alterations in plant morphology or development when compared with plants inoculated with the empty TRV vector. By contrast, silencing of *δ-COP*, *ARF1*, *CHC1* and *CHC2* led to morphological alterations, which became apparent between 7 and 9 dpi and were clearly manifested by 15 dpi (Fig. S11). These phenotypic alterations were characterized by reduced internodal elongation, leaf curling and chlorosis, and the onset of necrosis when silencing *CHC1* and *CHC2*.

In order to assess the effect of the silencing of the selected elements in the endomembrane trafficking system, we studied the localization of markers fused to GFP for different subcellular compartments: (1) the transmembrane domain of the rat α-2,6-sialyltransferase (STtmd) to mark the Golgi, (2) the syntaxin SYP41 to mark the TGN and (3) the vacuolar receptor BP80 to mark PVC/MVB. The third and fourth younger leaves from silenced plants were infiltrated with *Agrobacterium tumefaciens* cultures to express the organelle-specific fluorescent markers. Two days later, the fluorescent signal from markers was analysed by confocal laser scanning microscopy (CLSM; Fig. S12). As a control, the fluorescent markers were agroinfiltrated in *N. benthamiana* leaves from nonsilenced plants (inoculated with the empty TRV vector). The analysis was performed in plants silenced with six out of the eight genes selected (*δ-COP*, *ARF1*, *SAR1*, *SEC24*, *CHC2* and *AP-1γ*). *CHC1* was discarded, due to its functional redundancy with *CHC2* (Figs S8, S9), and *SYT1* was not included since it has been previously reported that Arabidopsis *syt1* knockout mutants only show severely altered phenotypes during salt stress (Benitez-Fuente & Botella, 2023). Representative images of all the results are shown in Fig. S13 and summarized in Table 3. The degree of silencing of each assayed gene was determined and the data for one representative replica are shown (Table S2).

Subcellular redistribution of the Golgi marker STtmd-GFP, primarily to the ER (Figs 2, S13, S14), was detected when the expression of any of the studied genes was reduced. This effect is likely due to the Golgi's central role as a crossroads organelle that organizes cargo sorting to various compartments. Among the silenced genes, *SAR1* reduction caused the most extensive disruption, also leading to a clear redistribution of the TGN marker (SYP41-GFP) into cytosolic strands and aggregates, as well as the MVB marker (BP80-GFP) to the ER (Figs 2, S14, S15). These results parallel those obtained with the GTPase-defective mutant Sar1p (H74L), which specifically inhibits COPII-mediated ER-to-Golgi trafficking. Overexpression of this mutant resulted in the redistribution of fluorescence to the ER, involving both the Golgi and vacuolar storage markers (Table S3). Intriguingly, although the *in silico* study with VIGS tool analysis predicted that the TRV-SAR1 VIGS construct could induce silencing in only four out of the 11 *N. benthamiana* homologues (Table 2), the significant relocalization of the markers suggests that SAR1 function was extensively impaired in the silenced plants. In Arabidopsis, all SAR1 family members are implicated in ER-to-Golgi trafficking and localized to ER exit sites (ERES) to mediate

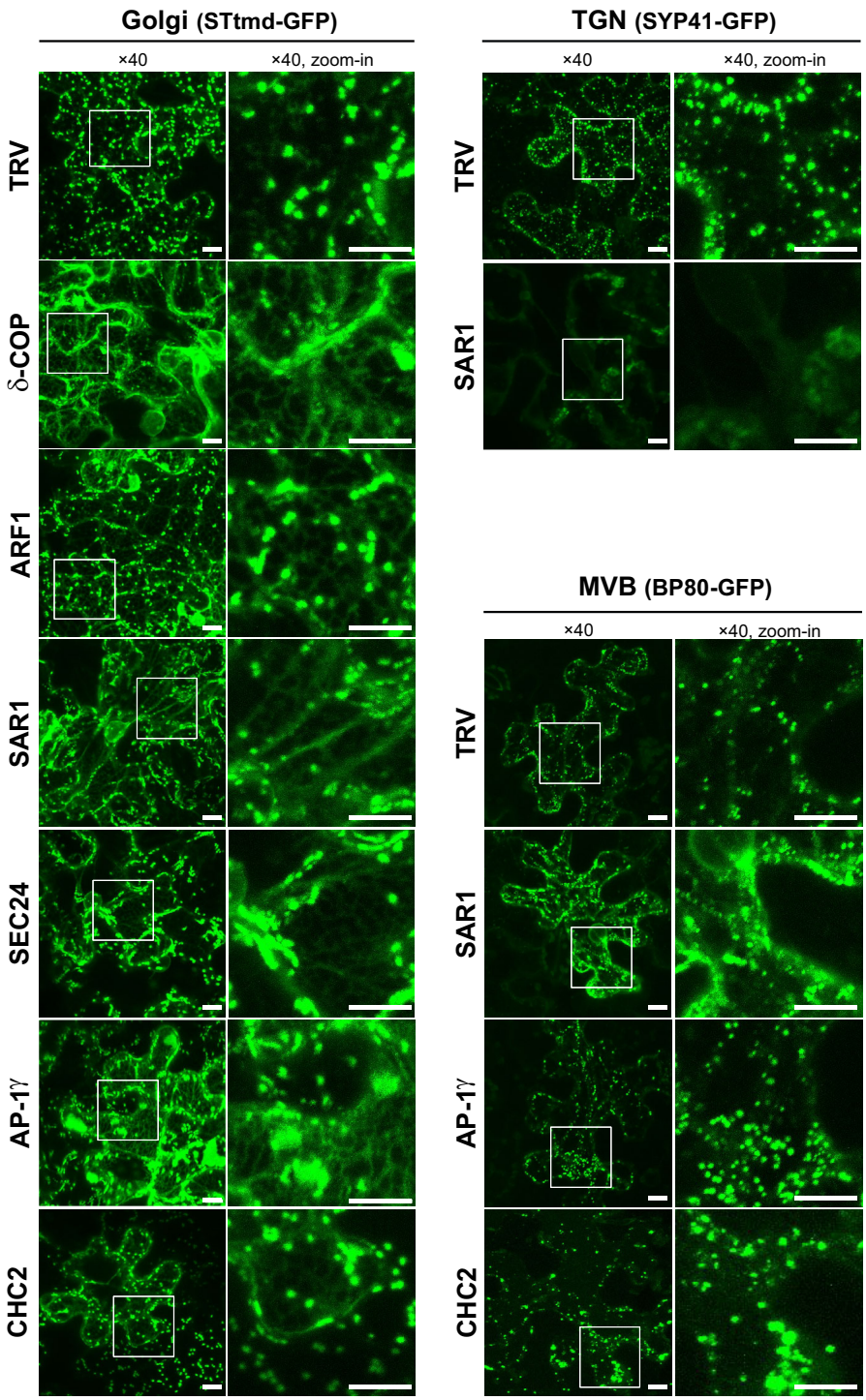

Fig. 2 Impact of *δ-COP*, *ARF1*, *SAR1*, SEC24, *AP-1γ* and *CHC2* silencing on the vesicle trafficking system. Confocal laser scanning microscopy (CLSM) images showing the subcellular localization in *Nicotiana benthamiana* leaves of STtmd-GFP (marker for Golgi), SYP41-GFP (marker for *trans*-Golgi network (TGN)) and BP80-GFP (maker for MVB) in leaves agroinfiltrated with the empty vector (TRV) or with the TRV constructs to silence the selected genes at 13 d postinfection. Bars, 10 μm. Experiments were repeated twice with similar results. Representative images from both experiments are shown. Gene silencing efficiency was determined by RT-qPCR (Table S2). TRV, tobacco rattle virus.

anterograde trafficking, differing in their cargo recognition specificity for proper ER-to-Golgi delivery (Hanton *et al.*, 2008; Zeng *et al.*, 2015; Feng *et al.*, 2017). We speculate that if vesicles from the ER are not delivered, the Golgi precursor Golgi entry core compartments (GECCO) would not be formed, leading to severe distortions of Golgi structures (Ito & Boutté, 2020) and an altered distribution of TGN and MVB markers.

Nonetheless, these effects on the TGN and MVB markers were not observed when *SEC24*, which encodes an essential anterograde trafficking factor forming adpator subunits of COPII vesicles, was knocked down (Fig. S13). The differential effects observed when silencing *SAR1* and *SEC24* genes could arise from two distinct mechanisms: functional redundancy among SEC24A homologues or a partial knockdown of *SEC24A* that remains insufficient to impair trafficking function, in contrast to the profound disruption caused by *SAR1* silencing. In Arabidopsis, three SEC24 paralogues (A–C) play distinct roles in vesicle trafficking (Faso *et al.*, 2009; Tanaka *et al.*, 2013). While SEC24A is

essential for plant viability (Faso *et al.*, 2009), SEC24B and SEC24C are crucial for gametogenesis but not required for plant survival, nor able to rescue *sec24a* mutants (Tanaka *et al.*, 2013; Chang *et al.*, 2022). Therefore, we speculate that these differences in *SAR1* and *SEC24* silencing are most likely due to an incomplete silencing of *SEC24* rather than paralogue-specific functional compensation.

On the contrary, the distribution of the MVB/PVC marker (BP80-GFP) was also altered by silencing of *AP-1γ* or *CHC2*, leading to its relocalization into large aggregates and to the ER, respectively (Figs 2, S16). The enlargement of MVBs in *CHC*-silenced plants is aligned with the central role of clathrins in the formation of most post-Golgi trafficking compartments (sorted in the TGN and MVBs), as well as in mediating endocytosis, secretion or vacuolar transport. Likewise, the pronounced effect on BP80 localization agreed with the role of the AP-1 complex in the vacuolar and secretory pathways (Law *et al.*, 2022; Shimizu & Uemura, 2022).

Surprisingly, *ARF1* silencing did not alter the distribution of TGN or MVB/PVC markers but specifically disrupted the localization of the Golgi marker (STmd-GFP; Figs S13, S14). This result was unexpected, as *ARF1* belongs to a complex gene family encoding GTPases critical for vesicle recruitment and formation at the Golgi, post-Golgi compartments and PM (Singh *et al.*, 2018). Consequently, *ARF1* knockdown was anticipated to impair TGN and MVB marker dynamics. Nonetheless, considering the large complexity of the *ARF1* gene family, it is very likely that some of *N. benthamiana ARF1* paralogues may not be targeted by our TRV-ARF1 construct, which would explain the wild type-like post-Golgi marker distributions.

To place our observations within a broader context, we compiled a supplementary table summarizing the documented effects on endomembrane function and marker localization when the expression of our selected genes in Arabidopsis was altered (Table S3). This comparison underscores both the similarities and differences with our findings and supports the interpretation that the observed phenotypes are consistent with perturbations of endomembrane trafficking pathways described in previous studies.

Impact of silencing the selected vesicle trafficking-related genes on TYLCSaV infection

To evaluate the impact of the silencing of the selected genes on endomembrane trafficking during the infection with geminiviruses, we used *2IRGFP N. benthamiana* plants, which enable viral replication tracking through GFP expression (Morilla *et al.*, 2006; Lozano-Durán *et al.*, 2011). Leaves were first infiltrated with TRV-derived silencing constructs to induce gene silencing, followed by inoculation with an infectious TYLCSaV clone in the stem directly above the infiltration site (Fig. 3a). As a control, TYLCSaV was inoculated into *2IRGFP* plants preinfiltrated with the empty TRV-based vector. GFP expression was monitored from 7 to 15 dpi. To evaluate the development of the infection, we implemented an index named replication-associated phenotype (RAP), scoring the plants from 0 to 3 according to the visually detected levels of GFP under UV light (Fig. 3b; Lozano-Durán *et al.*, 2011). A score of 0 was given to leaves that expressed no GFP at all, 1 to those leaves which showed GFP expression limited to the major veins of the leaf, 2 to those which had GFP not only in the major veins but also in some secondary veins and 3 when most of the leaf tissue was expressing GFP. The results are represented in Fig. 3c.

Silencing the two genes involved in the retrograde pathway (*δ-COP* and *ARF1*) or the structural components of the CCVs (*CHC1* and *CHC2*) severely impaired TYLCSaV infection. All silenced plants exhibited a RAP score of 0 throughout the experimental period, indicating that reduced expression of these genes completely disrupted viral infection. By contrast, silencing *AP-1γ*, a CCV adaptor subunit, accelerated infection progression at early stages, achieving GFP expression levels comparable to control plants at 12 dpi. Conversely, silencing *SYT1* or the anterograde route-involved genes (*SAR1* and *SEC24*) produced a delay in the infection development. However, *SAR1* and *SYT1* silenced plants reached TRV control levels from 13 dpi onward. Notably, *SEC24* silenced plants maintained reduced GFP expression levels throughout the infection, showing an average RAP index 40% lower than the TRV control plants at 15 dpi (1.47 vs 2.47, respectively; Fig. 3c).

To further characterize the impact of gene silencing on viral infection, total DNA was extracted from each plant (TRV-silenced and nonsilenced) at 15 dpi and viral DNA accumulation was determined using qPCR. The qPCR results largely corroborated the RAP data. Consistent with the absence of GFP fluorescence, silencing of *δ-COP*, *ARF1*, *CHC1* and *CHC2* nearly abolished TYLCSaV accumulation (Fig. 4). Conversely, *SAR1* silencing promoted a higher level of infection by tripling TYLCSaV accumulation as well as the silencing of *AP-1γ – a* component of a specific subset of CCVs – which strikingly increased viral DNA levels on average. By contrast, *SYT1* and *SEC24* silencing had no significant effect on the accumulation of viral DNA at 15 dpi. Quantification of the mRNA levels, in the same tissue used for viral DNA accumulation, confirmed the silencing of the target genes, as their expression levels were reduced to 45% and 14% of those detected in nonsilenced plants (Table S4).

Our findings demonstrate that the plant vesicular trafficking system plays a critical role in the viral infection cycle. To clarify whether silencing key trafficking genes inhibits viral replication, we performed a local infection assay in leaves. *N. benthamiana* plants were agroinfiltrated with the TRV constructs targeting the genes that impair viral systemic infection: *δ-COP*, *ARF1* and *CHC2*. Seven days postinoculation with the TRV-based VIGS constructs (a timepoint when the phenotypical defects of silenced plants started to be evident) leaves were agroinoculated with TYLCSaV, and viral DNA accumulation was quantified in the infiltrated leaf areas at 4 dpi (Fig. 5a). No significant differences in viral DNA levels were observed between silenced and TRV control plants (Fig. 5b), indicating that viral replication remains unaffected despite disruption of vesicular trafficking. mRNA quantification on the same tissue used to measure viral DNA accumulation, confirmed successful silencing of *δ-COP*, *ARF1* and *CHC2* (Table S5). The results indicate that replication of

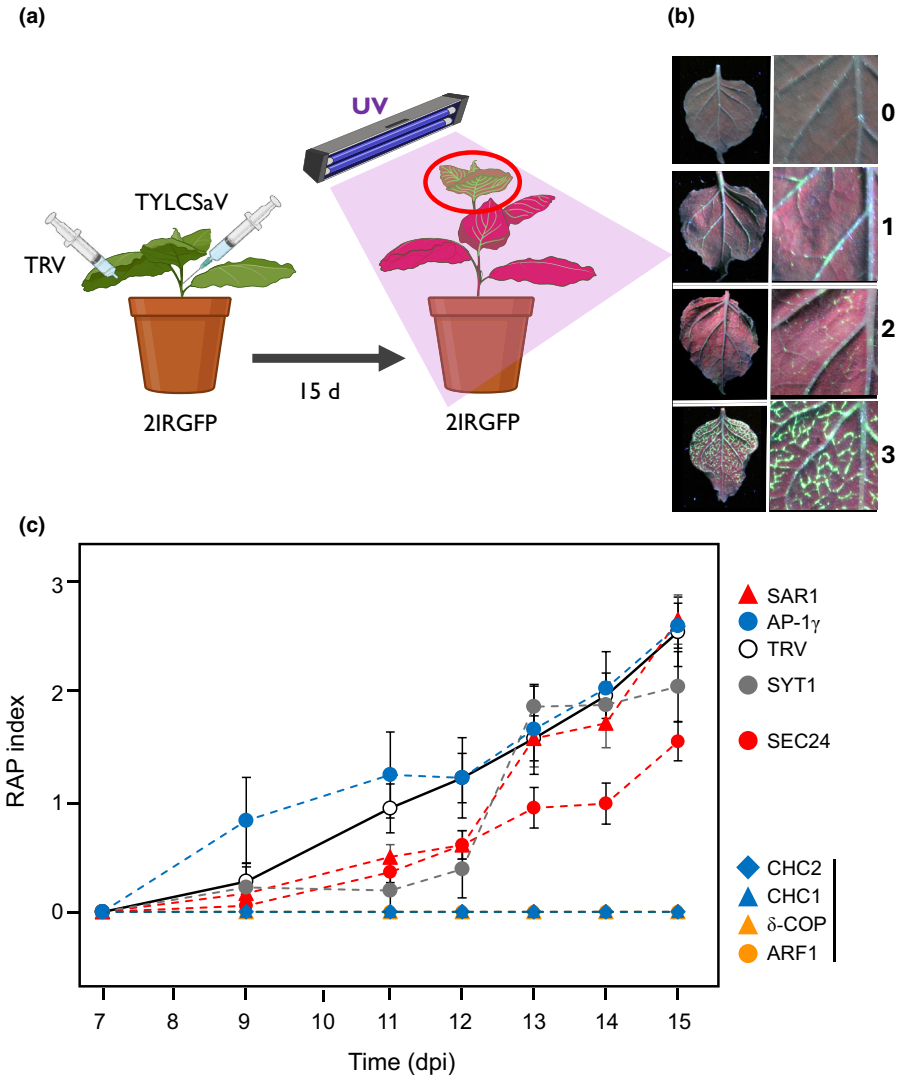

Fig. 3 Effect of silencing the selected vesicle trafficking-related genes during tomato yellow leaf curl Sardinia virus (TYLCSaV) infection. (a) *2IRGFP Nicotiana benthamiana* plants were co-inoculated with a TRV:Gene construct and TYLCSaV. GFP expression was daily monitored under UV light until 15 dpi (adapted from Lozano-Durán *et al*., 2011). (b) Scale of replication-associated phenotype (RAP) by which plants were classified during the monitoring. 0 = no GFP expression, 1 = GFP in major veins only, 2 = GFP in major and some secondary veins, 3 = GFP in most of the veins of the leaf. (c) Dynamics of the RAP phenotype in plants silenced for each of the selected genes in the 7–15 dpi period. Each point represents the average RAP score of 5 (AP-1γ and SYT1), 10 (δ-COP and ARF1) or 20 (CHC1, CHC2, SAR1 and SEC24) plants. Symbols of the genes that participate in the same type of vesicle coating formation are shown in the same colour. Error bars represent SE. dpi, d postinfection; GFP, green fluorescence protein; TRV, tobacco rattle virus.

TYLCSaV is not affected by the silencing of *ARF1*, *δ-COP* and *CHC2*. These findings demonstrate that TYLCSaV replication is independent of ARF1, δ-COP or CHC2 activity, suggesting that impaired systemic infection in silenced plants arises from postreplication defects.

Because impairment of systemic infection occurs in silenced plants affected in development, we cannot exclude the possibility that the reduced systemic spread might be a consequence of impaired phloem function. To test this, we performed CFDA assays to monitor phloem transport, which revealed no alteration in phloem conductivity in silenced plants (Fig. S17). *N. benthamiana* plants were agroinfiltrated with the TRV constructs targeting two of the genes that showed developmental effects when silenced (*δ-COP and ARF1*). Nine days postinoculation with the TRV-based VIGS constructs each source leaf was infiltrated with CDFA or water as a negative control, and the fluorescent signal was visualized and quantified in the source and the sink leaf and petiole at 3 h post infiltration. CFDA transport from source to sink leaves was unaffected in *ARF1*- and *δ-COP*-silenced plants, indicating that the reduction in systemic spread does not result from a general defect in phloem function but rather reflects a specific impairment in viral phloem uploading when these genes are silenced.

Virus-induced silencing of *δ-COP* and *ARF1* abolishes geminivirus infection but does not affect infection by the RNA virus PVX or the plant pathogenic bacterium *Pseudomonas syringae*

To assess the specificity of the retrograde pathway's role in systemic viral infection, we challenged *δ-COP*- and *ARF1*-silenced plants with other DNA and RNA viruses. Plants were inoculated with two additional geminiviruses – the begomovirus TYLCV and the curtovirus BCTV – as well as a recombinant RNA virus PVX, containing the GFP gene (PVX-GFP; Peart *et al*., 2002; Jaubert *et al*., 2011).

Total DNA (for geminiviruses) or RNA (for PVX-GFP) was extracted from apical leaves at 15 dpi and quantified via qPCR or RT-qPCR (Reverse transcription quantitative PCR), respectively. Consistent with the results obtained with TYLCSaV, *δ-COP* and

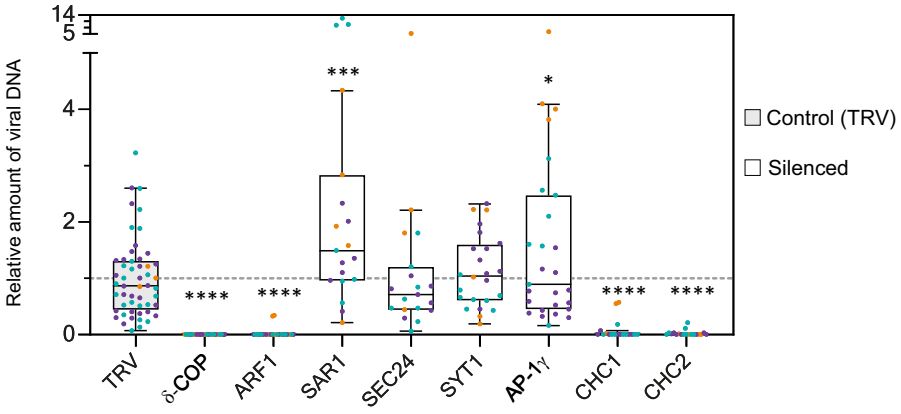

Fig. 4 Effect of virus-induced gene silencing of membrane trafficking-related genes on tomato yellow leaf curl Sardinia virus (TYLCSaV) accumulation. Relative amount of TYLCSaV DNA in the three most apical leaves of *Nicotiana benthamiana* plants co-infected with TYLCSaV and the respective TRV-derived silencing constructs or empty TRV as control. Viral DNA was measured by quantitative real-time PCR (qPCR) at 15 d postinfection in silenced (gene indicated between brackets) and nonsilenced (TRV) plants. Values represent the mean from 18 to 28 measurements for silenced plants and 52 for the nonsilenced ones as a negative control for gene silencing. Viral DNA levels were normalized to *NbACT* and are presented as relative quantities compared with the nonsilenced control (TRV, set to 1). Whiskers were calculated according to the Tukey approach, extending to the most extreme data points within 1.5 × IQR from the lower and upper quartiles. Asterisks indicate samples showing a statistically significant difference with the TRV control (no silencing) according to a Student's *t*-test (****, *P*-value < 0.0001; ***, *P*-value < 0.001; *, *P*-value < 0.05). The experiment was conducted in three independent replicates, yielding consistent results, which are distinguished by dot colours (orange, purple and blue). IQR, interquartile range; TRV, tobacco rattle virus.

ARF1 silencing drastically reduced TYLCV and BCTV DNA accumulation; however, it had no significant effect on PVX RNA levels (Fig. 6a).

To evaluate the retrograde pathway's role in the infection by extracellular pathogens, *δ-COP*- and *ARF1*-silenced *N. benthamiana* plants were inoculated with *Pseudomonas syringae* pv *tomato* DC3000 *ΔhopQ1-1*, a strain pathogenic in *N. benthamiana* (Wei *et al.*, 2007). Bacterial growth was measured at 3 dpi, with no significant differences observed between silenced and TRV control plants (Fig. 6b).

Taken together, these findings demonstrate that an intact retrograde trafficking pathway is specifically required for geminivirus infection, but not for PVX or bacterial infection.

Discussion

The endomembrane system plays a dual role in the viral life cycle, both providing the machinery and membranes necessary for viral infection and contributing to plant immunity mainly through autophagy (Yang *et al.*, 2020; Lozano-Durán, 2024; Yagyu & Yoshimoto, 2024). Previous evidence from our group demonstrated that silencing one of the genes of the COPI complex, *δ-COP*, almost completely blocked TYLCSaV infection, indicating that the host endomembrane trafficking network is essential for geminiviral infection (Lozano-Durán *et al.*, 2011). To further analyse the involvement of vesicle trafficking during infection, we have performed a functional analysis silencing essential genes for the function of the complexes of the three types of vesicles (COPI, COPII and CCVs) that are involved, respectively, in the Golgi-to-ER retrograde pathway (*δ-COP* and *ARF1*), the ER-to-Golgi anterograde pathway (*SAR1* and *SEC24*) and post-Golgi trafficking (*AP-1γ*, *CHC1*, *CHC2* and again *ARF1*). Additionally, we also included a host factor essential for functional membrane contact sites formation (*SYT1*).

The results obtained here confirm that vesicle trafficking plays a very important role in the infection by geminiviruses, since silencing six of the eight studied genes alters the viral accumulation in the plant. Only in two cases, *SYT1* and *SEC24*, silencing did not have any impact on the infection. In the case of *SYT1*, this result contrasts with that previously obtained with the bipartite begomovirus CabLCV in Arabidopsis, since a knockdown mutation of *SYT1* compromised viral cell-to-cell movement and delayed the infection (Lewis & Lazarowitz, 2010; Uchiyama *et al.*, 2014). The fact that the MP from CabLCV interacts with SYT1 led the authors to suggest that this interaction directs the MP to dock at plasmodesmata for the viral intercellular transport. Considering that TYLCSaV monopartite genome does not encode a homologue to MP, we cannot rule out the possibility that SYT1 may be specifically involved in the movement of bipartite begomiviruses.

Silencing of the other genes affects the ability of TYLCSaV to infect *N. benthamiana* plants allowing greater virus accumulation (*SAR1* and *AP-1γ*) or strongly blocking infection (*δ-COP*, *ARF1*, *CHC1* and *CHC2*). We believe that these seemingly contradictory results can be explained, respectively, by the inhibition of different vesicular trafficking-dependent processes: (1) protein degradation by autophagy or vacuolar transport and (2) clathrin-mediated endo-exocytosis.

It is important to note that although the VIGS fragments were carefully designed to maximize specificity within each targeted gene family, the possibility of off-target silencing cannot be completely excluded, particularly through the generation of secondary

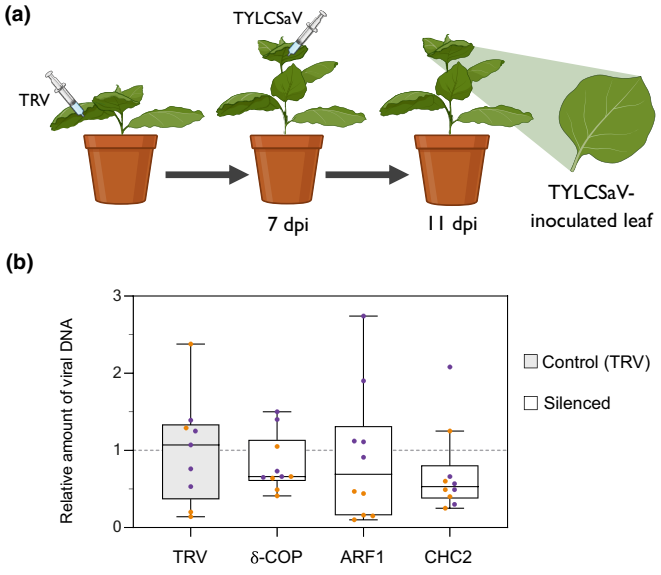

Fig. 5 Replication of tomato yellow leaf curl Sardinia virus (TYLCSaV) is not affected in *δ-COP*-, *ARF1*- or *CHC*-silenced plants. (a) Schematic representation of the experimental setup used to determine the capability of TYLCSaV to replicate in silenced *Nicotiana benthamiana* plants. (b) Relative amount of viral DNA in the TYLCSaV infiltrated leaves that were silenced for *δ-COP*, *ARF1* and *CHC2* genes or nonsilenced (TRV) at 11 d postinfection. Viral DNA levels were normalized to *NbACT* and are presented as relative quantities compared with the nonsilenced control (TRV, set to 1). Whiskers were calculated according to the Tukey approach, extending to the most extreme data points within 1.5 × IQR from the lower and upper quartiles. No statistically significant differences were observed, as determined by Student's *t*-test. The experiment was conducted in two independent replicates, yielding consistent results, which are distinguished by dot colours (orange and purple). dpi, d postinoculation; IQR, interquartile range; TRV, tobacco rattle virus.

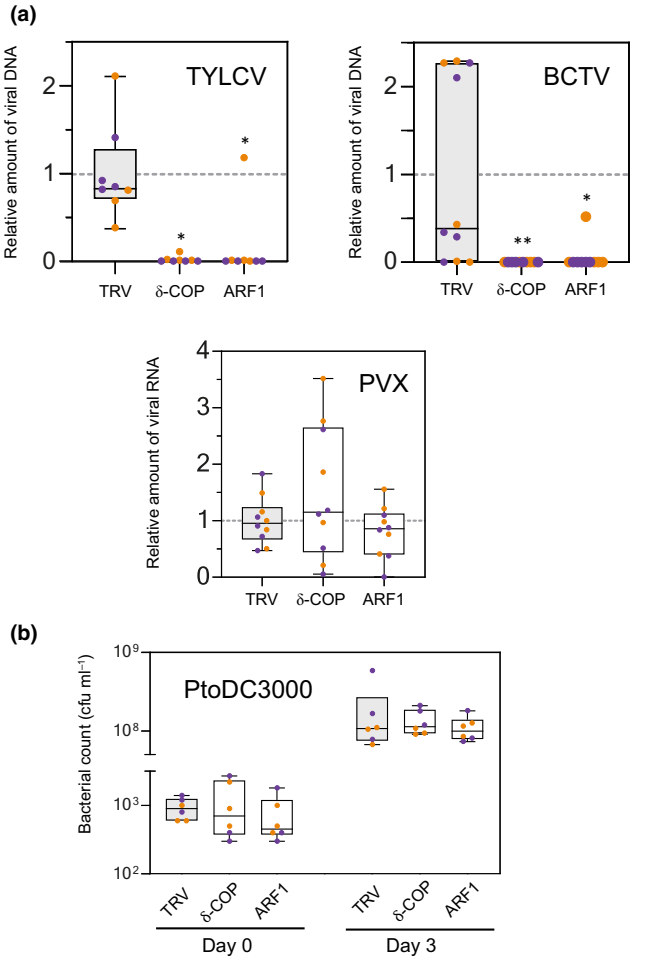

Fig. 6 Silencing of *δ-COP* and *ARF1* abolishes geminivirus infection but does not alter potato virus X (PVX) or *Pseudomonas syringae* pv *tomato* DC3000 Δ*hopQ1-1* infection. (a) Relative amount of TYLCV DNA, BCTV DNA (qPCR) or PVX RNA (RT-qPCR) in *Nicotiana benthamiana* infected plants that were silenced for *δ-COP* or *ARF1* genes or nonsilenced (TRV) at 15 dpi. Viral DNA levels were normalized to *NbACT* and presented as relative quantities compared with the nonsilenced control (TRV, set to 1). Whiskers were calculated according to the Tukey approach, extending to the most extreme data points within 1.5 × IQR from the lower and upper quartiles. Asterisks indicate samples showing a statistically significant difference compared with TRV control (**, *P*-value < 0.01; *, *P*-value < 0.05) according to a Student's *t*-test. The experiment was conducted in two independent replicates, yielding consistent results, which are distinguished by dot colours (orange and purple). (b) Ten-day-silenced *δ-COP* or *ARF1 N. benthamiana* plants were infiltrated with *P. syringae* pv *tomato* DC3000 Δ*hopQ1-1* at 5 × 10 CFU ml^{-1}. The growth of the bacteria was determined at 0 dpi and 3 dpi. No statistically significant differences were observed, as determined by Student's *t*-test. The experiment was conducted in two independent replicates, yielding consistent results, which are distinguished by dot colours (orange and purple). CFU, colony-forming units; dpi, d postinfection; IQR, interquartile range; TRV, tobacco rattle virus.

siRNAs by transitivity (de Felippes *et al.*, 2020). This limitation implies that the phenotypes we describe most likely reflect the combined contribution of multiple paralogues within a gene family rather than the function of a single gene, and thus should be interpreted as family-wide effects until validated by complementation or other genetic approaches. Future studies employing specific mutants will be required to disentangle the individual roles of each family member in the observed phenotype.

SAR1 and AP-1γ participate in defence mechanisms that undermine the viral infection

Autophagy plays a significant antiviral role in the host's innate and adaptive plant immune responses (Yang *et al.*, 2020; Wu *et al.*, 2022; Zhang *et al.*, 2023). Numerous studies have described autophagy as a defence mechanism employed by plants against geminiviruses, among other strategies, through the degradation of viral proteins. Thus, geminiviral βC1 and Rep proteins that interact with autophagy-related gene 8 protein (ATG8) are degraded by autophagy (Haxim *et al.*, 2017; Li *et al.*, 2020) and, in accordance, a Rep mutation in the putative interaction motif with ATG8 enhanced virus pathogenicity (Li *et al.*, 2020). Besides, disruption of the autophagy by silencing either *ATG5* or *ATG7* enhances geminivirus accumulation, while autophagy induction impairs geminiviral infection (Haxim *et al.*, 2017).

Autophagy function requires the formation of large double-membrane vesicles, called autophagosomes, that deliver cytoplasmic components to the vacuole. The formation of those vesicles requires the recruitment of autophagy-related (ATG) proteins and the membrane trafficking machinery from the secretory pathway, including the COPII vesicles and the post-Golgi pathways, which provide membranes for autophagosome formation (Davis *et al.*, 2017; Li *et al.*, 2022).

In Arabidopsis, different COPII components are involved in separate steps of autophagosome biogenesis. SAR1D interacts with the ATG8 isoform ATG8e and the reduction in its activity affects the autophagic flux (Zeng *et al.*, 2021). SAR1B, another SAR paralogue, appears to have a role later than SAR1D (Kim *et al.*, 2022), indicating that COPII machinery is required for autophagy function. We consequently propose that *SAR1* silencing in *N. benthamiana* could impair autophagy; therefore allowing an increase in the viral accumulation.

Plant CCVs mainly function to sort *de novo* synthesized proteins from the TGN to PM for secretion or into MVB leading to vacuoles to constitute the vacuolar pathway. Besides, they are also involved in internalizing integral membrane proteins located on the PM into TGN in a mode of endocytosis (Paez Valencia *et al.*, 2016). The clathrin coat is mainly composed of a heterotetrameric adaptor protein (AP) complex together with a structure called the triskelion, comprised of three clathrin heavy chains and three light chains. The AP complex has five variants (AP-1 to AP-5), each comprising heterotetrameric polypeptides including two large subunits, a single medium and a single small one. These subunits work together to recognize specific signals on cargo proteins, bind to the cargo and assist in the recruitment of clathrins and other proteins necessary for vesicle formation. Each AP complex has been shown to function in protein trafficking at distinct locations. AP-1γ is one of the proteins of the AP-1 complex that mediates clathrin-dependent trafficking at the TGN to PM and vacuoles (Law *et al.*, 2022). AP-1γ drives the transport to the tonoplast of proteins by recognizing a dileucine-based sorting sequence (Wang *et al.*, 2014; Law *et al.*, 2022). Interestingly, we have noticed the CP of TYLCSaV contains a putative dileucine motif ENALLL at the C-terminus of the protein (aa 225 to 230) that is conserved in all begomoviral CPs (Fig. S18). During infection, the CP of TYLCV, located at the nucleus and cytoplasm, is degraded as a defence mechanism by protease digestion, 26S proteasome degradation and autophagy (Gorovits *et al.*, 2013, 2014, 2016). It would therefore be possible that CP transport to the vacuole for its degradation could be dependent on AP-1γ recognition of the ENALLL motif of CP. If so, silencing of *AP-1γ* would impair this transport, boosting the viral accumulation. These results suggest an antiviral effect of the vacuolar pathway, which could degrade viral components or proviral factors.

Clathrin-mediated endo-exocytosis: COPI and CCV-mediated trafficking are required for geminiviral infection

Silencing of *δ-COP*, *ARF1* and clathrin-coding genes almost completely abolished the virus detection in the apical leaves of infected plants. Even though δ-COP, CHC1 and CHC2 are indirectly related by ARF1, there is no clear direct functional link among them. In eukaryotes, clathrins and ARF1 are involved in the formation of CCVs at post-Golgi transport routes (endocytosis, secretion and vacuolar trafficking), while δ-COP and ARF1 function together in the formation of COPI vesicles. Although COPI vesicles are primarily involved in retrograde transport from the Golgi to the ER, COPI disruption could directly affect Golgi function in a manner similar to clathrin silencing, as it plays a crucial role in establishing the specific protein composition of all membrane organelles. Besides, in mammals and yeast, it has been described that several COPI subunits seem to be also involved in endosomal functions (Gu *et al.*, 1997; Gabriely *et al.*, 2007; Xu *et al.*, 2017), opening up the possibility that silencing of the COPI and CCV elements is altering common pathways, as it was also suggested by the fact that silenced plants showed similar morphological alterations.

Whatever the processes impaired by silencing these genes might be, our results indicate that they are not affecting the replication of geminiviruses (local infection; Fig. 5b) and therefore point to a suppression of their movement in the plant. The mechanisms involved do not alter infection of the RNA virus used (PVX) and neither affect the growth of *P. syringae* bacteria. Despite the co-occurrence of the abolishment of geminiviral infection and the developmental alterations observed when *δ-COP*, *ARF1* and clathrin genes were silenced, our results indicate that the vascular system of these plants is still functional, as CFDA transport was not affected (Fig. S17), PVX was still able to systemically infect plants and an acid fuchsin dye was able to reach apical leaves even when both genes were silenced (data not shown). According to our results, the reduced systemic spread is most likely due to direct effects on long-distance transport through the phloem. Given that *N. benthamiana* is an apoplastic-loading species, in which the phloem is relatively isolated from surrounding mesophyll cells, we propose that the observed effects more likely reflect limitations in phloem uploading and subsequent long-distance transport. Although the data pointed to defects in post-Golgi transport pathways (exocytic, endocytic or vacuolar) as responsible for the effect in this viral movement, additional work will be required to identify the specific processes affected by the gene silencing that are essential for geminiviruses to be able to infect the plant systemically.

Notably, during the preparation of this manuscript, Zhao *et al.* reported findings consistent with ours: silencing of the tomato δ-COP gene also impairs TYLCV infection in tomato. In addition, they further demonstrated that silencing two other COPI complex subunits, β-COP and ε-COP, significantly reduces TYLCV infection, whereas overexpressing β-COP via a PVX vector increases viral titre in infected plants. Finally, Zhao *et al.* proposed that COPI complexes mediate the targeting of the TYLCV C4 protein to chloroplasts and promote chloroplast clustering around the nucleus, proposing a model in which COPI components facilitate geminivirus infection by enabling C4 relocalization to chloroplasts.

However, our results with TYLCSaV cannot be fully explained by this chloroplast-targeting mechanism, since the C4 proteins of TYLCSaV and TYLCV differ in their subcellular localization

dynamics. Although both C4 proteins associate with the PM and chloroplasts, the TYLCV C4 protein which is predominantly PM-bound in noninfected cells relocates to chloroplasts upon infection. By contrast, TYLCSaV C4 is consistently detected in both compartments at comparable levels, even when transiently expressed in *N. benthamiana* leaves in the absence of viral infection (Fig. S19). Unlike the COPI-dependent relocalization of TYLCV C4 from the PM to the chloroplast (Zhao *et al.*, 2024), the localization of TYLCSaV C4 within chloroplasts of uninfected plants appears to be independent of COPI-mediated transport, as it is unaffected by either BFA treatment or δ-COP silencing (Fig. S19). Finally, silencing other host trafficking genes not involved in COPI-mediated transport, such as CHC or ARF1, produces a similarly strong inhibition of TYLCSaV infection as δ-COP silencing. This finding suggests that the pronounced antigeminiviral phenotype observed is due to a general disruption of the host vesicle transport machinery rather than exclusively to the mislocalization of C4 away from chloroplasts.

Conclusions

The endomembrane trafficking dissection shown in the present work lays one of the foundation stones in identifying the relevance of vacuolar trafficking for geminivirus infection. On the one hand, we speculate that the vacuolar pathway and MVBs might act as sorting hubs exerting dual roles in geminiviral infection, eliciting both defence responses against viruses (most likely autophagy-mediated) and facilitating viral movement through recycling routes or endocytosis. On the other hand, we hypothesize that endocytosis and retrograde pathways may constitute essential processes for successful systemic viral infection. The use of receptor-mediated endocytosis to enter host cells is well established for animal viruses (Helenius, 2018; Roth *et al.*, 2021), but in plants, its role during viral infections remains majorly unknown and only a few examples have been described, centred mainly on turnip mosaic virus and cauliflower mosaic virus (Carluccio *et al.*, 2014; Wu *et al.*, 2020). Interestingly, endocytosis has also been demonstrated to play an important role in the trafficking of geminiviruses through the midgut cells of their insect vectors (Pan *et al.*, 2017; Xia *et al.*, 2018; Wang *et al.*, 2019; Zhao *et al.*, 2020). Considering that endocytic machinery is majorly conserved throughout kingdoms, a similar role of endocytosis during geminivirus infections in plants is conceivable and would open new thrilling questions in the field.

Acknowledgements

This work was funded by the Plan Nacional I + D + i, Ministerio de Economía y Competitividad (Agencia Estatal de Investigación), Spain (PID2022-139376OB-C31), and a PhD Fellowship (FPU20/03715) from Ministerio de Ciencia, Innovación y Universidades. Funding for open access charge: Universidad de Málaga/CBUA. The funders had no role in study design, data collection and analysis, decision to publish, or preparation of the manuscript.

Competing interests

None declared.

Author contributions

ERB, VP, AGC, RL-D and PC-Q conceived and designed the experiments. PC-Q performed most of the experiments. TR-D, TJ-G, NJA and JPS helped with the experiments. PC-Q, ERB, AGC and PM-M analysed and discussed the data. ERB, PM-M and AGC wrote the manuscript. All the authors have read, revised and approved the paper. PC-Q and PM-M contributed equally to this work.

ORCID

Eduardo R. Bejarano https://orcid.org/0000-0002-4806-253X
Pepe Cana-Quijada https://orcid.org/0000-0001-8655-8694
Araceli G. Castillo https://orcid.org/0000-0003-3990-5475
Tamara Jiménez-Góngora https://orcid.org/0000-0001-9831-251X
Rosa Lozano-Durán https://orcid.org/0000-0001-7348-8842
Pablo Morales-Martínez https://orcid.org/0000-0001-5140-4986
José Antonio Navarro https://orcid.org/0000-0003-2844-9742
Jessica Pérez-Sancho https://orcid.org/0000-0002-6201-3240
Vicente Pallás https://orcid.org/0000-0003-4954-989X
Tábata Rosas-Díaz https://orcid.org/0000-0002-4338-6711

Data availability

All data are available in the manuscript and its Supporting Information. Genomic sequences for viral species used in this work are indexed and stored in the GenBank Database: TYLCSaV (GenBank accession: L27708), TYLCV (GenBank accession: AJ489258) and BCTV (GenBank accession: NC001412).

References

Aniento F, Sánchez de Medina Hernández V, Dagdas Y, Rojas-Pierce M, Russinova E. 2022. Molecular mechanisms of endomembrane trafficking in plants. *Plant Cell* **34**: 146–173.

Ausubel M, Brent R, Kingston RE, Moore DD, Seidman JG, Smith JA, Struhl K. 1998. *Current protocols in molecular biology*. New York, NY, USA: John Wiley & Sons.

Benitez-Fuente F, Botella MA. 2023. Biological roles of plant synaptotagmins. *European Journal of Cell Biology* **102**: 151335.

Berg S, Kutra D, Kroeger T, Straehle CN, Kausler BX, Haubold C, Schiegg M, Ales J, Beier T, Rudy M *et al.* 2019. ilastik: interactive machine learning for (bio)image analysis. *Nature Methods* **16**: 1226–1232.

Brandizzi F. 2018. Transport from the endoplasmic reticulum to the Golgi in plants: where are we now? *Seminars in Cell & Developmental Biology* **80**: 94–105.

Brandizzi F, Barlowe C. 2013. Organization of the ER-Golgi interface for membrane traffic control. *Nature Reviews. Molecular Cell Biology* **14**: 382–392.

Briddon RW, Watts J, Markham PG, Stanley J. 1989. The coat protein of beet curly top virus is essential for infectivity. *Virology* **172**: 628–633.

Cabanillas DG, Jiang J, Movahed N, Germain H, Yamaji Y, Zheng H, Laliberté JF. 2018. Turnip mosaic v irus uses the SNARE protein VTI11 in an unconventional route for replication vesicle trafficking. *Plant Cell* **30**: 2594–2615.

Cadena-Ramos AI, De-la-Peña C. 2024. Picky eaters: selective autophagy in plant cells. *The Plant Journal* **117**: 364–384.

Carluccio AV, Zicca S, Stavolone L. 2014. Hitching a ride on vesicles: cauliflower mosaic virus movement protein trafficking in the endomembrane system. *Plant Physiology* **164**: 1261–1270.

Carvalho CM, Fontenelle MR, Florentino LH, Santos AA, Zerbini FM, Fontes EPB. 2008. A novel nucleocytoplasmic traffic GTPase identified as a functional target of the bipartite geminivirus nuclear shuttle protein. *The Plant Journal* **55**: 869–880.

Chang M, Wu SZ, Ryken SE, O'Sullivan JE, Bezanilla M. 2022. COPII Sec23 proteins form isoform-specific endoplasmic reticulum exit sites with differential effects on polarized growth. *Plant Cell* **34**: 333–350.

Chi Y, Pan LL, Liu SS, Mansoor S, Wang XW. 2021. Implication of the whitefly protein Vps twenty associated 1 (Vta1) in the transmission of cotton leaf curl multan virus. *Microorganisms* **9**: 304.

Coemans B, Takahashi Y, Berberich T, Ito A, Kanzaki H, Matsumura H, Saitoh H, Tsuda S, Kamoun S, Sági L *et al.* 2008. High-throughput *in planta* expression screening identifies an ADP-ribosylation factor (ARF1) involved in non-host resistance and R gene-mediated resistance. *Molecular Plant Pathology* **9**: 25–36.

Cuppels DA. 1986. Generation and characterization of Tn5 insertion mutations in *Pseudomonas syringae* pv. tomato. *Applied and Environmental Microbiology* **51**: 323–327.

Davis S, Wang J, Ferro-Novick S. 2017. Crosstalk between the secretory and autophagy pathways regulates autophagosome formation. *Developmental Cell* **41**: 23–32.

Elmer JS, Sunter G, Gardiner WE, Brand L, Browning CK, Bisaro DM, Rogers SG. 1988. Agrobacterium-mediated inoculation of plants with tomato golden mosaic virus DNAs. *Plant Molecular Biology* **10**: 225–234.

Faso C, Chen YN, Tamura K, Held M, Zemelis S, Marti L, Saravanan RS, Hummel E, Kung L, Miller E *et al.* 2009. A missense mutation in the Arabidopsis COPII coat protein Sec24A induces the formation of clusters of the endoplasmic reticulum and Golgi apparatus. *Plant Cell* **21**: 3655–3671.

de Felippes FF, McHale M, Doran RL, Roden S, Eamens AL, Finnegan EJ, Waterhouse PM. 2020. The key role of terminators on the expression and post-transcriptional gene silencing of transgenes. *The Plant Journal* **104**: 96–112.

Feng QN, Song SJ, Yu SX, Wang JG, Li S, Zhang Y. 2017. Adaptor protein-3-dependent vacuolar trafficking involves a subpopulation of COPII and HOPS tethering proteins. *Plant Physiology* **174**: 1609–1620.

Fiallo-Olivé E, Lett JM, Martin DP, Roumagnac P, Varsani A, Zerbini FM, Navas-Castillo J. 2021. ICTV virus taxonomy profile: Geminiviridae 2021. *Journal of General Virology* **102**: 001696.

Fiallo-Olivé E, Navas-Castillo J. 2023. Begomoviruses: what is the secret(s) of their success? *Trends in Plant Science* **28**: 715–727.

Gabriely G, Kama R, Gerst JE. 2007. Involvement of specific COPI subunits in protein sorting from the late endosome to the vacuole in yeast. *Molecular and Cellular Biology* **27**: 526–540.

Gao YQ, Chao DY. 2022. Localization and circulation: vesicle trafficking in regulating plant nutrient homeostasis. *The Plant Journal* **112**: 1350–1363.

Gebbie LK, Burn JE, Hocart CH, Williamson RE. 2005. Genes encoding ADP-ribosylation factors in *Arabidopsis thaliana* L. Heyn.; genome analysis and antisense suppression. *Journal of Experimental Botany* **56**: 1079–1091.

González Solís A, Berryman E, Otegui MS. 2022. Plant endosomes as protein sorting hubs. *FEBS Letters* **596**: 2288–2304.

Gorovits R, Fridman L, Kolot M, Rotem O, Ghanim M, Shriki O, Czosnek H. 2016. Tomato yellow leaf curl virus confronts host degradation by sheltering in small/midsized protein aggregates. *Virus Research* **213**: 304–313.

Gorovits R, Moshe A, Ghanim M, Czosnek H. 2014. Degradation mechanisms of the tomato yellow leaf curl virus coat protein following inoculation of tomato plants by the whitefly *Bemisia tabaci*. *Pest Management Science* **70**: 1632–1639.

Gorovits R, Moshe A, Kolot M, Sobol I, Czosnek H. 2013. Progressive aggregation of Tomato yellow leaf curl virus coat protein in systemically infected tomato plants, susceptible and resistant to the virus. *Virus Research* **171**: 33–43.

Gouveia-Mageste BC, Martins LGC, Dal-Bianco M, Machado JPB, Da Silva JCF, Kim AY, Yazaki J, Dos Santos AA, Ecker JR, Fontes EPB. 2021. A plant-specific syntaxin-6 protein contributes to the intracytoplasmic route for the begomovirus CabLCV. *Plant Physiology* **187**: 158–173.

Gu F, Aniento F, Parton RG, Gruenberg J. 1997. Functional dissection of COP-I subunits in the biogenesis of multivesicular endosomes. *The Journal of Cell Biology* **139**: 1183–1195.

Hanton SL, Chatre L, Matheson LA, Rossi M, Held MA, Brandizzi F. 2008. Plant Sar1 isoforms with near-identical protein sequences exhibit different localisations and effects on secretion. *Plant Molecular Biology* **67**: 283–294.

Haxim Y, Ismayil A, Jia Q, Wang Y, Zheng X, Chen T, Qian L, Liu N, Wang Y, Han S *et al.* 2017. Autophagy functions as an antiviral mechanism against geminiviruses in plants. *eLife* **6**: e23897.

Helenius A. 2018. Virus entry: looking back and moving forward. *Journal of Molecular Biology* **430**: 1853–1862.

Hu S, Li Y, Shen J. 2020. A diverse membrane interaction network for plant multivesicular bodies: roles in proteins vacuolar delivery and unconventional secretion. *Frontiers in Plant Science* **11**: 425.

Ito Y, Boutté Y. 2020. Differentiation of trafficking pathways at Golgi entry core compartments and post-Golgi subdomains. *Frontiers in Plant Science* **11**: 609516.

Jackson CL, Ménétrey J, Sivia M, Dacks JB, Eliáš M. 2023. An evolutionary perspective on Arf family GTPases. *Current Opinion in Cell Biology* **85**: 102268.

Jaubert M, Bhattacharjee S, Mello AFS, Perry KL, Moffett P. 2011. ARGONAUTE2 mediates RNA-silencing antiviral defenses against potato virus X in Arabidopsis. *Plant Physiology* **156**: 1556–1564.

Kim JH, Lee HN, Huang X, Jung H, Otegui MS, Li F, Chung T. 2022. FYVE2, a phosphatidylinositol 3-phosphate effector, interacts with the COPII machinery to control autophagosome formation in Arabidopsis. *Plant Cell* **34**: 351–373.

Krapp S, Schuy C, Greiner E, Stephan I, Alberter B, Funk C, Marschall M, Wege C, Bailer SM, Kleinow T *et al.* 2017. Begomoviral movement protein effects in human and plant cells: Towards new potential interaction partners. *Viruses* **9**: 334.

Law KC, Chung KK, Zhuang X. 2022. An update on coat protein complexes for vesicle formation in plant Post-Golgi trafficking. *Frontiers in Plant Science* **13**: 826007.

Lee MH, Min MK, Lee YJ, Jin JB, Shin DH, Kim DH, Lee K-H, Hwang I. 2002. ADP-ribosylation factor 1 of Arabidopsis plays a critical role in intracellular trafficking and maintenance of endoplasmic reticulum morphology in Arabidopsis. *Plant Physiology* **129**: 1507–1520.

Lewis JD, Lazarowitz SG. 2010. Arabidopsis synaptotagmin SYTA regulates endocytosis and virus movement protein cell-to-cell transport. *Proceedings of the National Academy of Sciences, USA* **107**: 2491–2496.

Li B, Zeng Y, Jiang L. 2022. COPII vesicles in plant autophagy and endomembrane trafficking. *FEBS Letters* **596**: 2314–2323.

Li F, Zhang M, Zhang C, Zhou X. 2020. Nuclear autophagy degrades a geminivirus nuclear protein to restrict viral infection in solanaceous plants. *New Phytologist* **225**: 1746–1761.

Livak KJ, Schmittgen TD. 2001. Analysis of relative gene expression data using real-time quantitative PCR and the 2(-Delta Delta C(T)) Method. *Methods* **25**: 402–408.

Lozano-Durán R. 2024. Viral recognition and evasion in plants. *Annual Review of Plant Biology* **75**: 655–677.

Lozano-Durán R, Rosas-Díaz T, Luna AP, Bejarano ER. 2011. Identification of host genes involved in geminivirus infection using a reverse genetics approach. *PLoS ONE* **6**: e22383.

Lukowitz W, Mayer U, Jürgens G. 1996. Cytokinesis in the Arabidopsis embryo involves the syntaxin-related KNOLLE gene product. *Cell* **84**: 61–71.

Luo PM, Boyce M. 2019. Directing traffic: regulation of COPI transport by post-translational modifications. *Frontiers in Cell and Developmental Biology* **7**: 190.

Morilla G, Castillo AG, Preiss W, Jeske H, Bejarano ER. 2006. A versatile transreplication-based system to identify cellular proteins involved in geminivirus replication. *Journal of Virology* **80**: 3624–3633.

Morilla G, Janssen D, García-Andrés S, Moriones E, Cuadrado IM, Bejarano ER. 2005. Pepper (*Capsicum annuum*) is a dead-end host for tomato yellow leaf curl virus. *Phytopathology* **95**: 1089–1097.

Muthamilarasan M, Mangu VR, Zandkarimi H, Prasad M, Baisakh N. 2016. Structure, organization and evolution of ADP-ribosylation factors in rice and foxtail millet, and their expression in rice. *Scientific Reports* **6**: 24008.

Naramoto S, Kleine-Vehn J, Robert S, Fujimoto M, Dainobu T, Paciorek T, Ueda T, Nakano A, Van Montagu MCE, Fukuda H *et al.* 2010. ADP-ribosylation factor machinery mediates endocytosis in plant cells. *Proceedings of the National Academy of Sciences, USA* **107**: 21890–21895.

Navarro JA, Sanchez-Navarro JA, Pallas V. 2019. Key checkpoints in the movement of plant viruses through the host. In: Kielian M, Mettenleiter TC, Roossinck M, eds. *Advances in virus research, vol. 104*. Cambridge, MA, USA: Academic Press, 1–64.

Oñate-Sánchez L, Vicente-Carbajosa J. 2008. DNA-free RNA isolation protocols for *Arabidopsis thaliana*, including seeds and siliques. *BMC Research Notes* **1**: 93.

Paez Valencia J, Goodman K, Otegui MS. 2016. Endocytosis and endosomal trafficking in plants. *Annual Review of Plant Biology* **67**: 309–335.

Pan LL, Chen QF, Zhao JJ, Guo T, Wang XW, Hariton-Shalev A, Czosnek H, Liu SS. 2017. Clathrin-mediated endocytosis is involved in tomato yellow leaf curl virus transport across the midgut barrier of its whitefly vector. *Virology* **502**: 152–159.

Peart JR, Cook G, Feys BJ, Parker JE, Baulcombe DC. 2002. An EDS1 orthologue is required for N-mediated resistance against tobacco mosaic virus. *The Plant Journal* **29**: 569–579.

Pimpl P, Hanton SL, Taylor JP, Pinto-daSilva LL, Denecke J. 2003. The GTPase ARF1p controls the sequence-specific vacuolar sorting route to the lytic vacuole. *Plant Cell* **15**: 1242–1256.

Pitzalis N, Heinlein M. 2017. The roles of membranes and associated cytoskeleton in plant virus replication and cell-to-cell movement. *Journal of Experimental Botany* **69**: 117–132.

Ranawaka B, An J, Lorenc MT, Jung H, Sulli M, Aprea G, Roden S, Llaca V, Hayashi S, Asadyar L *et al.* 2023. A multi-omic *Nicotiana benthamiana* resource for fundamental research and biotechnology. *Nature Plants* **9**: 1558–1571.

Ratcliff F, Martin-Hernandez AM, Baulcombe DC. 2001. Technical advance: tobacco rattle virus as a vector for analysis of gene function by silencing. *The Plant Journal* **25**: 237–245.

Rodriguez-Peña R, El Mounadi K, Garcia-Ruiz H. 2021. Changes in subcellular localization of host proteins induced by plant viruses. *Viruses* **13**: 677.

Roth AN, Aravamudhan P, Fernández de Castro I, Tenorio R, Risco C, Dermody TS. 2021. Ins and outs of reovirus: vesicular trafficking in viral entry and egress. *Trends in Microbiology* **29**: 363–375.

Sambrook J, Russell DW. 2001. *Molecular cloning: a laboratory manual*. New York, NY, USA: Cold Spring Harbor Laboratory Press.

Schindelin J, Arganda-Carreras I, Frise E, Kaynig V, Longair M, Pietzsch T, Preibisch S, Rueden C, Saalfeld S, Schmid B *et al.* 2012. Fiji: an open-source platform for biological-image analysis. *Nature Methods* **9**: 676–682.

Shimizu Y, Uemura T. 2022. The sorting of cargo proteins in the plant *trans*-Golgi network. *Frontiers in Plant Science* **13**: 957995.

Singh MK, Jürgens G. 2018. Specificity of plant membrane trafficking – ARFs, regulators and coat proteins. *Seminars in Cell & Developmental Biology* **80**: 85–93.

Singh MK, Richter S, Beckmann H, Kientz M, Stierhof YD, Anders N, Fäßler F, Nielsen M, Knöll C, Thomann A *et al.* 2018. A single class of ARF GTPase activated by several pathway-specific ARF-GEFs regulates essential membrane traffic in Arabidopsis. *PLoS Genetics* **14**: e1007795.

Takeuchi M, Ueda T, Yahara N, Nakano A. 2002. Arf1 GTPase plays roles in the protein traffic between the endoplasmic reticulum and the Golgi apparatus in tobacco and Arabidopsis cultured cells. *The Plant Journal* **31**: 499–515.

Tanaka H, Nodzyński T, Kitakura S, Feraru MI, Sasabe M, Ishikawa T, Kleine-Vehn J, Kakimoto T, Friml J. 2014. BEX1/ARF1A1C is required for BFA-sensitive recycling of PIN auxin transporters and auxin-mediated development in Arabidopsis. *Plant and Cell Physiology* **55**: 737–749.

Tanaka Y, Nishimura K, Kawamukai M, Oshima A, Nakagawa T. 2013. Redundant function of two Arabidopsis COPII components, AtSec24B and AtSec24C, is essential for male and female gametogenesis. *Planta* **238**: 561–575.

Uchiyama A, Shimada-Beltrán H, Levy A, Zheng JY, Javia PA, Lazarowitz SG. 2014. The Arabidopsis synaptotagmin SYTA regulates the cell-to-cell movement of diverse plant viruses. *Frontiers in Plant Science* **5**: 584.

Van der Verren SE, Zanetti G. 2023. The small GTPase Sar1, control centre of COPII trafficking. *FEBS Letters* **597**: 865–882.

Vernoud V, Horton AC, Yang Z, Nielsen E. 2003. Analysis of the small GTPase gene superfamily of Arabidopsis. *Plant Physiology* **131**: 1191–1208.

Wang H, Liu Y, Zhang L, Kundu JK, Liu W, Wang X. 2019. ADP ribosylation factor 1 facilitates spread of wheat dwarf virus in its insect vector. *Cellular Microbiology* **21**: e13047.

Wang X, Cai Y, Wang H, Zeng Y, Zhuang X, Li B, Jiang L. 2014. *Trans*-Golgi network-located AP1 gamma adaptins mediate dileucine motif-directed vacuolar targeting in Arabidopsis. *Plant Cell* **26**: 4102–4118.

Wei CF, Kvitko BH, Shimizu R, Crabill E, Alfano JR, Lin NC, Martin GB, Huang HC, Collmer A. 2007. A *Pseudomonas syringae* pv. tomato DC3000 mutant lacking the type III effector HopQ1-1 is able to cause disease in the model plant *Nicotiana benthamiana*. *The Plant Journal* **51**: 32–46.

Wu G, Cui X, Dai Z, He R, Li Y, Yu K, Bernards M, Chen X, Wang A. 2020. A plant RNA virus hijacks endocytic proteins to establish its infection in plants. *The Plant Journal* **101**: 384–400.

Wu M, Wei H, Tan H, Pan S, Liu Q, Bejarano ER, Lozano-Durán R. 2021. Plant DNA polymerases α and δ mediate replication of geminiviruses. *Nature Communications* **12**: 2780.

Wu W, Luo X, Ren M. 2022. Clearance or hijack: universal interplay mechanisms between viruses and host autophagy from plants to animals. *Frontiers in Cellular and Infection Microbiology* **11**: 786348.

Xia WQ, Liang Y, Chi Y, Pan LL, Zhao J, Liu SS, Wang XW. 2018. Intracellular trafficking of begomoviruses in the midgut cells of their insect vector. *PLoS Pathogens* **14**: e1006866.

Xu J, Scheres B. 2005. Dissection of Arabidopsis ADP-RIBOSYLATION FACTOR 1 function in epidermal cell polarity. *Plant Cell* **17**: 525–536.

Xu P, Hankins HM, MacDonald C, Erlinger SJ, Frazier MN, Diab NS, Piper RC, Jackson LP, MacGurn JA, Graham TR. 2017. COPI mediates recycling of an exocytic SNARE by recognition of a ubiquitin sorting signal. *eLife* **6**: e28342.

Yagyu M, Yoshimoto K. 2024. New insights into plant autophagy: molecular mechanisms and roles in development and stress responses. *Journal of Experimental Botany* **75**: 1234–1251.

Yang M, Ismayil A, Liu Y. 2020. Autophagy in plant-virus interactions. *Annual Review of Virology* **7**: 403–419.

Yorimitsu T, Sato K, Takeuchi M. 2014. Molecular mechanisms of Sar/Arf GTPases in vesicular trafficking in yeast and plants. *Frontiers in Plant Science* **5**: 411.

Yuen ELH, Shepherd S, Bozkurt TO. 2023. Traffic control: subversion of plant membrane trafficking by pathogens. *Annual Review of Phytopathology* **61**: 325–350.

Zeng Y, Chung KP, Li B, Lai CM, Lam SK, Wang X, Cui Y, Gao C, Luo M, Wong KB *et al.* 2015. Unique COPII component AtSar1a/AtSec23a pair is required for the distinct function of protein ER export in *Arabidopsis thaliana*. *Proceedings of the National Academy of Sciences, USA* **112**: 14360–14365.

Zeng Y, Li B, Ji C, Feng L, Niu F, Deng C, Chen S, Lin Y, Cheung KCP, Shen J *et al.* 2021. A unique AtSar1D-AtRabD2a nexus modulates autophagosome biogenesis in *Arabidopsis thaliana*. *Proceedings of the National Academy of Sciences, USA* **118**: e2021293118.

Zeng Y, Liang Z, Liu Z, Li B, Cui Y, Gao C, Shen J, Wang X, Zhao Q, Zhuang X *et al.* 2023. Recent advances in plant endomembrane research and new microscopical techniques. *New Phytologist* **240**: 41–60.

Zhang J, Ma M, Liu Y, Ismayil A. 2023. Plant defense and viral counter-defense during plant–geminivirus interactions. *Viruses* **15**: 510.

Zhao W,Ji Y, Zhou Y, Wang X. 2024. Geminivirus C4/AC4 proteins hijack cellular COAT PROTEIN COMPLEX I for chloroplast targeting and viral infections. *Plant physiology* **196**: 1826–1839.

Zhao J, Lei T, Zhang XJ, Yin TY, Wang XW, Liu SS. 2020. A vector whitefly endocytic receptor facilitates the entry of begomoviruses into its midgut cells via binding to virion capsid proteins. *PLoS Pathogens* **16**: e1009053.

Supporting Information

Additional Supporting Information may be found online in the Supporting Information section at the end of the article.

Fig. S1 Orthologue search in *Nicotiana benthamiana* and *in silico* silencing analysis.

Fig. S2 Analysis and characterization of *δ-COP* silencing in *Nicotiana benthamiana*.

Fig. S3 Analysis and characterization of *ARF1* silencing in *Nicotiana benthamiana*.

Fig. S4 Analysis and characterization of *SAR1* silencing in *Nicotiana benthamiana*.

Fig. S5 Analysis and characterization of *SEC24* silencing in *Nicotiana benthamiana*.

Fig. S6 Analysis and characterization of *SYT1* silencing in *Nicotiana benthamiana*.

Fig. S7 Analysis and characterization of *AP-1γ* silencing in *Nicotiana benthamiana*.

Fig. S8 Analysis and characterization of *CHC1* silencing in *Nicotiana benthamiana*.

Fig. S9 Analysis and characterization of *CHC2* silencing in *Nicotiana benthamiana*.

Fig. S10 Design of TRV-derived constructs for silencing.

Fig. S11 Phenotypes of *Nicotiana benthamiana* plants at 15 d postinfection inoculated with empty TRV-based vector or TRV construct designed to silence the indicated vesicle trafficking-related-genes.

Fig. S12 Strategy used to study the impact of silencing the targeted genes on different compartments of the vesicle trafficking system.

Fig. S13 Impact of *δ-COP*, *ARF1*, *SAR1*, *SEC24*, *AP-1γ* and *CHC2* silencing on the vesicle trafficking system.

Fig. S14 Quantification of the impact of *δ-COP*, *ARF1*, *SAR1*, *CHC2*, *SEC24* and *AP-1γ* silencing on the Golgi marker STtmd-GFP.

Fig. S15 Quantification of the impact of *SAR1* silencing on the TGN marker SYP41-GFP.

Fig. S16 Quantification of the impact of *SAR1*, *CHC2* and *AP-1γ* silencing on the MVB marker BP80-GFP.

Fig. S17 CFDA transport in source and sink leaves of VIGS-silenced plants.

Fig. S18 Identification of a dileucine ENALLL motif in several geminiviral coat protein sequences.

Fig. S19 Effect of BFA treatment and *δ–COP* silencing on subcellular localization of C4 from TYLCSaV.

Table S1 List of primers used in this work.

Table S2 Measurement of targeted gene silencing in endomembrane trafficking markers CLSM analysis.

Table S3 Effect of mutations in COPII, COPI, ARF1, AP-1 subunits and clathrin, on endomembrane markers in *Arabidopsis thaliana*.

Table S4 Measurement of targeted gene silencing in TYLCSaV systemic infection assays.

Table S5 Measurement of targeted gene silencing in TYLCSaV replication assays.

Please note: Wiley is not responsible for the content or functionality of any Supporting Information supplied by the authors. Any queries (other than missing material) should be directed to the *New Phytologist* Central Office.